scientific reports

Check for updates

OPEN

Decadal (2012–2023) account of spatio-temporal variability in satellite-detected biomass fires on Indian landmass and their fire radiative power

Deepanjan Majumdar

Worldwide escalation in wildfire incidences calls for continuous monitoring and early detection of fires to strengthen regional fire combating strategies. Inter-annual variability in fire count and Fire Radiative Power (FRP), spatial spread of fires in the most active seasons during 2012–2023 on Indian landmass are reported. Fire data is extracted from 375 m active fire detection product of Visible Infrared Imaging Radiometer Suite (VIIRS) hosted by Suomi National Polar-orbiting Partnership. In every fire-year (March–February), constructed from the month of remarkable escalation in fires, fires were most populated in March or April in summer and November in winter. The yearly sum of fire spots ranged from 492,282 (2013) to 731,154 (2021). Inter-annual fire count trend grew at a rate of 10,794 per year, excluding COVID years of 2020 and 2021. Many cities with > 0.1 million population are located within or adjacent to the fire hot spots (20 km × 20 km grids), implying possibility of some impacts of seasonal fires both within and outside Wildfire Urban Interphases (WUIs). The study highlights the urgency of streamlining interventions to minimize wildfire incidences in order to protect forests, habitats, biodiversity, ecosystem services, human lives and property and minimize carbon loss, air pollution, perturbations in regional meteorology and radiative forcing.

Keywords Crop residue burning, Fire count, Fire spot, Remote sensing, Sen's slope, VIIRS

Forest fire, grassland fire, crop-residue burning (CRB) are prevalent worldwide since long[1–3]. Fires in Savannah, forests, shifting cultivation, wood fuel combustion and CRB contributed about 50, 24, 10, 11, and 5%, respectively, in biomass fires occurred in tropic during late 1970's itself[4]. Cunningham et al.[5] reports that frequency of extreme events increased by about 2.2-fold during 2003–2023, in which the last 7 years included the 6 most extreme ones. In spite of the fact that the total burnt area on earth may be declining, their study reports that fire behaviour is on a worsening trend in several regions, particularly the boreal and temperate conifer biomes, with serious implications on carbon storage and human exposure to wildfire disasters. In the recent 2023–2024 fire season, an area of 3.9×10^6 sq. km. was under fire and fire carbon (C) emission was to the tune of 2.4 Pg C. Noteworthy wildfire episodes were recorded in Canada, Greece, Western Amazonia, Hawaii and Chile[6]. UNEP[7] has expressed concerns on escalating forest and peatland fires that are threatening the extensive ecosystem services received from these regions. Increasing trend in the proportion of areas under high-intensity fires is reported from boreal forests of Siberia, including the Arctic zone during the past decade[8]. Further, Australia is frequently devastated by wildfires, with the most recent episodes occurring during 2019–2020, costing in excess $4.4 billion in losses[9]. The evidences on the integral link of human health to wildfires is continuously emerging and has been reviewed recently[10].Approximately 730 Tg biomass was estimated to have combusted annually in Asia during early parts of the decade of 2000 in which India's CRB had a share of about 18%[11]. In recent times, CRB alone accounted for about 25% of total biomass burnt worldwide[12,13]. The short interval of about 2–3 weeks in between rice harvesting and sowing of wheat have instigated farmers to burn paddy residues during Oct–Nov in India to clear fields for sowing[14]. Indian Agricultural Research Institute reports combustion of about 14 million tons (Mt) (about 63.6%) out of about 22 Mt paddy stubble generated in India each year[15]. But, in spite of a longer interval of about 46–48 days in between wheat harvesting and sowing of rice during April–May[16], wheat stubbles

Kolkata Zonal Centre, CSIR-National Environmental Engineering Research Institute (CSIR-NEERI), i-8, Sector C, EKADP, E.M. Bypass, Kolkata, India. email: d_majumdar@neeri.res.in

are also found being put on fire in recent times[17]. Two important agricultural states of India, Haryana and Punjab, contributed about 48% to CRB during the first decade of twenty-first century[18]. Apart from CRB, severe incidences of fire are also reported from dry deciduous forests in India while other types of forests were found to be comparatively less prone to heavy fires[19]. More than 36% of India's forest cover is prone to frequent forest fires while about 4% and 6% of forest cover are extremely and highly fire prone, respectively[20]. On the other hand, forest fires are regularly spotted on Indian landmass, mostly during summer. According to Forest Survey of India (FSI), 52,785 forest fires were detected by Moderate Resolution Imaging Spectroradiometer (MODIS) while Visible Infrared Imaging Radiometer Suite (VIIRS) was able to detect 345,989 forest fires during November 2020 to June 2021[21]. The escalation in forest and biomass fires in specific parts of India has been flagged earlier but fire data had largely been extracted from Along Track Scanning Radiometer (ATSR) or MODIS[22–25] that did not have comparable ability to acquire data on small fires like the Suomi-VIIRS has[26].

Documented incidences of human influence in causing deliberate and sometimes inadvertent wildfires are concerning[27]. In mountain regions of North–eastern India, slash and burn agriculture is practiced for long to clear forest land for agriculture, leading to arson in forest patches[28]. Banerjee[29] found that wind speed, temperature, closeness to roads and tree cover are the crucial limiting factors in wildfires incidences in Sikkim Himalaya of India. Other factors like altitude, forests composition, precipitation and population density of trees also influence wildfires[30]. Fire Radiative Power (FRP), a measure of instant radiative energy emanating from fires[31], is depicted as pixel-integrated FRP in Mega Watts (MW). It is an important variable to characterize the extent of fire[32].

Biomass fires, remotely detected by sensors mounted on satellites, is an extremely useful method to study wildfires[3,33,34]. The data on thermal hotspots and fire activity reported by VIIRS and MODIS are known to conform in hotspot detection but a better spatial resolution of 375 m in VIIRS ensures better response for small fires[35]. The active fire data (375 m) reported by VIIRS that embarked on its mission on the polar orbiting Suomi National Polar-orbiting Partnership (Suomi-NPP) in 2012, complement the 1 km MODIS data acquired from Terra and Aqua satellites.

Wildfires and CRB lead to emissions of PM_{10}, $PM_{2.5}$, black carbon (BC) and several gases[35–37] Episodic biomass burning are also linked to substantial regional air pollution[38]. Further, biomass fires are known to alter landscapes[39], cause hydrologic and geomorphic changes[40], perturb local and regional meteorology[41], change surface albedo in post-fire periods[42],reduce organic soil carbon and nitrogen[43], destruct forest biomass[41,44] and flora and fauna[45], enforce long-term climate change[46], making biomass and wildfires extremely hostile to environment. Wildfires have strong influence on forest succession and play an active role in the replacement of existing tree species by new ones with different adaptation behaviour[47]. Microbial succession in soil in the aftermath of forest fires is also widely known[48,49]. Wildfires are also damaging to the delivery of ecosystem services like timber supply, animal hunting, honey, mushroom, resin and other forest product supply by inflicting losses in forest canopy, forest products, habitat and biodiversity[50–52]. Fires also limit human access to forests, affecting livelihoods. Forests repeatedly destroyed by fires reportedly had lesser woody surface fuels and tree seedling densities as compared to forests experiencing only a sole and recent wildfire. Also, repeatedly burnt areas may recover differently than once-burnt areas, leading to alternative ecosystem structure[53]. It is therefore crucial to monitor historical and also, near real time (NRT) fire incidences on regular basis to counter recurrent fires and protect environment and natural resources.

This study was envisaged to analyze and report trends in fire counts and FRPs during 2012–2023, right from the beginning of data acquisition by Suomi-VIIRS up to 2023, considering the presence of a highly 'fire sensitive' I-Band with 375 m spatial resolution (at nadir) that can detect 'small' active fires with < 1 MW FRP in VIIRS's[34]. This study gives insight on (i) temporal variability and trends of biomass fire spots on Indian landmass(ii) seasonality in the fire incidents (iii) fires hot spots in 20 km × 20 km grids vis a vis the populated urban centres. The spatial spread and clustering of biomass fires in 'hot spots' over Indian landmass vis a vis seasons and populated cities, will help understand potential impacts of emanating smoke and heat on urban centres.

Methods

Study area

Indian landmass (in between 8° 4′ and 37° 6′ north latitudes and 68° 7′ and 97° 25′ east longitudes), consisting of 28 states and 8 Union Territories[54], covering an area of about 32,87,263 sq. km[55] ,was chosen as the study area. Indian landmass measures about 3214 km (north–south) and about 2933 km (east–west). India had 275 cities with > 1 lakh (> 0.1 million) population as per last population census conducted in 2011.

Fire and FRP data retrieval

Active fire spots captured by VIIRS on NASA/NOAA Suomi-National Polar-orbiting Partnership (Suomi NPP) satellite and processed by NASA's Fire Information Resource Management System (FIRMS) were extracted and analyzed for every month and year during 2012 to 2023. All the active fire spot data points recorded by VIIRS from the very first day of transmission from the S-NPP satellite in 2012 and archived in NASA-FIRMS Near Real-Time (NRT) active fire data product (375 m spatial resolution), were collected (https://firms.modaps.eosdis.nasa.gov). Subsequently, information on select parameters viz. geographical coordinates of fire spots, data acquisition date and time, levels of confidence in fire detection (low, nominal, high) and FRP of each fire was extracted from the collected database for detailed analysis and interpretation. In VIIRS, the acquired fire data is screened by a confidence algorithm in which detection confidence levels are set to 'low' (l), 'nominal' (n) and 'high' (h) for designating the quality of individual fire pixels that helps exclude false positive fire occurrences (https://data-nifc.opendata.arcgis.com/datasets/esri2::satellite-viirs-thermal-hotspots-and-fire-activity/about). To ensure incorporation of fewer false alarms in analysis, use of only nominal- and high-confidence fire pixels are prescribed, treating the low-confidence fire pixels as 'no fire'. On the other hand, maximum fire detectibility is

ensured when all three classes of fire pixels are considered[56]. In this study, all fires including l, n and h confidence levels were analyzed and reported to ensure maximum fire detectability. A certain fire may not get detected by a satellite, if (i) the fire started and ended outside the time frame of satellite overpass (ii) the fire is masked by cloud cover or tree canopy or heavy smoke (iii) when instruments develop glitches (iv) when the fire is too small or too cool to be detected. The onboard bow-tie deletion algorithm in VIIRS helps minimize detection of duplicate fire spots between adjacent scans at off-nadir position, resulting in fewer repeat fire detections than MODIS[57]. Apart from these general limitations of satellite remote sensing, VIIRS has the following specific limitations in fire detection: (i) Early afternoon orbit of VIIRS leads to large temporal separation between same-day data acquisitions[58] (ii) During daytime, potential false alarms are witnessed due to reflected solar radiation from solar panels, hot and bright surfaces, sun glint from small lakes/ponds and clouds. In night, false alarms include hot smoke plumes and reflected solar energy from cloud tops near the terminator[59]. However, Data verification and validation for VIIRS performed at selected sites across the globe, including specific field campaigns in small-to-medium size (< 500 ha) fires[60], showed a good agreement with VIIRS daytime and night-time fire data[34], showcasing the reliability of VIIRS as an efficient wildfire sensor.

The MODIS (Aqua and Terra combined) fire spots were also extracted from FIRMS product parallelly with VIIRS, for the purpose of presenting an inter-comparison of fire spots retrieved by the two instruments.

Data analysis

The fire counts recorded by VIIRS over 2012–2023 were extracted and the numbers of active fires in the most active months were analyzed. The Indian 'fire-year' cycle was constructed from the monthly variation in fire incidences in every year, following the concept proposed by Boschetti and Roy[61] that inculcates the logic of calculating a 12 month 'fire-year' cycle from the month of significant escalation in number of wildfires. The concept of fire-year was invoked in this study after preliminary analysis of historical fire data (2012–2023) over India. A 'fire year' incorporates a 12 month period, starting from the month of remarkable escalation in fire activity up to the completion of 12 months which may or may not coincide with a calendar year. Therefore, based on wildfire activities, a fire year may be different in different parts of the world. The authors proposed the concept specifically for studying inter-annual variability of fire activity and found that a March–February 'Fire Year' was suitable for studying global fire activity. For the sake of a wider understanding, the 'Fire Year' may be likened to a 'Fire Period' or a 'Fire Season'. The respective FRPs (MW) of fires were also extracted and analyzed. Further, inter-annual trends of yearly total fire count, median FRPs and annual sum FRPs of active fires were analyzed and assessed for inter-relationships by Ordinary Least Square (OLS) Method and coefficient of determination (R^2) was tested for statistical significance. The year-wise trends of yearly total fire counts, yearly median FRPS and total yearly sum of FRPs over 2012 to 2023 were also analyzed by Sen's nonparametric slope estimation methods. The COVID years of 2020 and 2021 were ignored for studying the inter-annual trends, considering potential impacts of perturbation in anthropogenic movements and activities during these two years on fires. The true slope of trends were estimated by Sen's nonparametric method in which the slope is estimated as the median of all pair-wise slopes between each pair of points in the data set[62,63]. This method has advantages like allowing missing values and non-inclusion of data of any particular distribution. Also, Sen's method is known to be not remarkably impacted by single data errors or outliers[64]. Frequency analysis of fire counts in select FRP ranges over the entire study period was conducted to understand the distribution pattern of fire counts under various FRP classes. Cluster analysis by Ward's Method was performed on the year-wise datasets (n = 12 months under each year) on total fire counts and sum FRPs to identify statistically similar or dissimilar years in terms of total fire counts and sum FRPs, respectively. Ward's Method, also known as Ward's minimum variance method, is one of the agglomerative hierarchial approaches used for cluster analysis and is known to be the most suitable for quantitative variables. This approach analyzes the variance of clusters and minimizes within-cluster variance[65].

Spatial distribution of active fire spots in months of highest occurrence in summer (March or April, as found through fire data analysis) and winter (November, as found through fire data analysis) were mapped on Indian landmass by generating shape files from fire coordinates extracted from FIRMS fire product and integrating the layers onto the shape file of India having first and second levels of administrative divisions (country and state borders). Fire density maps were prepared for the months of highest occurrences in summer and winter i.e. March and November of 2022 and March or April and November of 2023 in 20 km × 20 km grids, to delineate gridded fire hot spots over Indian landmass. The density maps were prepared on a GIS platform by dividing the entire study area into 20 km × 20 km grids followed by geometric processing of number of fire spots appearing in each grid and selective colour marking of grids by creating fire-spot number bins. The shape file of Indian cities having more than 1 lakh population (> 0.1 million) was prepared by extracting the city coordinates reported in India's last population census database conducted in 2011 and overlaid on fire density maps. These maps facilitated visual assessment of proximity of these busy urban centres to the fire hot spots of various intensities (i.e. with different classes of fire counts), developed in 20 × 20 sq. km. grids. The major cities and towns within the seasonal hot spots were labeled for easy identification.

Results and discussions

Suomi-VIIRS detected far higher number of fires than what Terra and Aqua MODIS together did (Table 1). The numbers of fires detected with nominal and high confidence levels by VIIRS were in the range of 82.1–84.2% of all fires in the calendar years of 2012 to 2023 while in MODIS, the fires detected with > 50% confidence level were 79.1–81% of total fire counts. The temporal variation in monthly total fire counts during 2012–2023 is presented in Fig. 1**,** showing wide temporal variation in monthly total fire counts over the study period. The summer fire count started to increase remarkably from March every year, peaking either in March itself (2012, 2013, 2015, 2016, 2018, 2021, 2022) or in April (2014, 2017, 2019, 2020, 2023), subsequently declining to reach low numbers by July with ensuing monsoon. At the onset of winter, fire count started to increase again from October onwards,

	VIIRS			MODIS			
Calendar year	Annual total number of all fires (A)	Annual total number of fires detected with n and h degrees of confidence	% fires detected with n and h degrees of confidence levels	Annual total number of all fires (B)	Annual total number of fires detected with > 50% confidence level	% fire detected with > 50% confidence level	Excess number of fires detected by VIIRS in the year
	(A)	(B)	(B/A)*100	(C)	(D)	(D/C)*100	(A–C)
2012	588,000	493,565	83.9	93,150	74,187	79.6	494,850
2013	496,054	409,216	82.5	71,173	56,901	79.9	424,881
2014	542,478	450,899	83.1	76,416	60,748	79.5	466,062
2015	484,215	403,725	83.4	68,433	54,385	79.5	415,782
2016	681,135	562,590	82.6	88,809	70,826	79.8	592,326
2017	603,490	495,432	82.1	82,545	65,614	79.5	520,945
2018	650,012	539,112	82.9	91,110	72,888	80.0	558,902
2019	536,536	442,642	82.5	75,502	61,163	81.0	461,034
2020	488,717	411,650	84.2	76,021	60,549	79.6	412,696
2021	771,277	644,390	83.5	111,267	88,751	79.8	660,010
2022	590,369	486,533	82.4	81,525	65,777	80.7	508,844
2023	578,591	479,962	83.0	78,425	62,061	79.1	500,166

Table 1. Inter-comparison of yearly (calendar-year) fire counts retrieved by SUOMI-VIIRS and MODIS (Aqua and Terra combined) over Indian landmass.

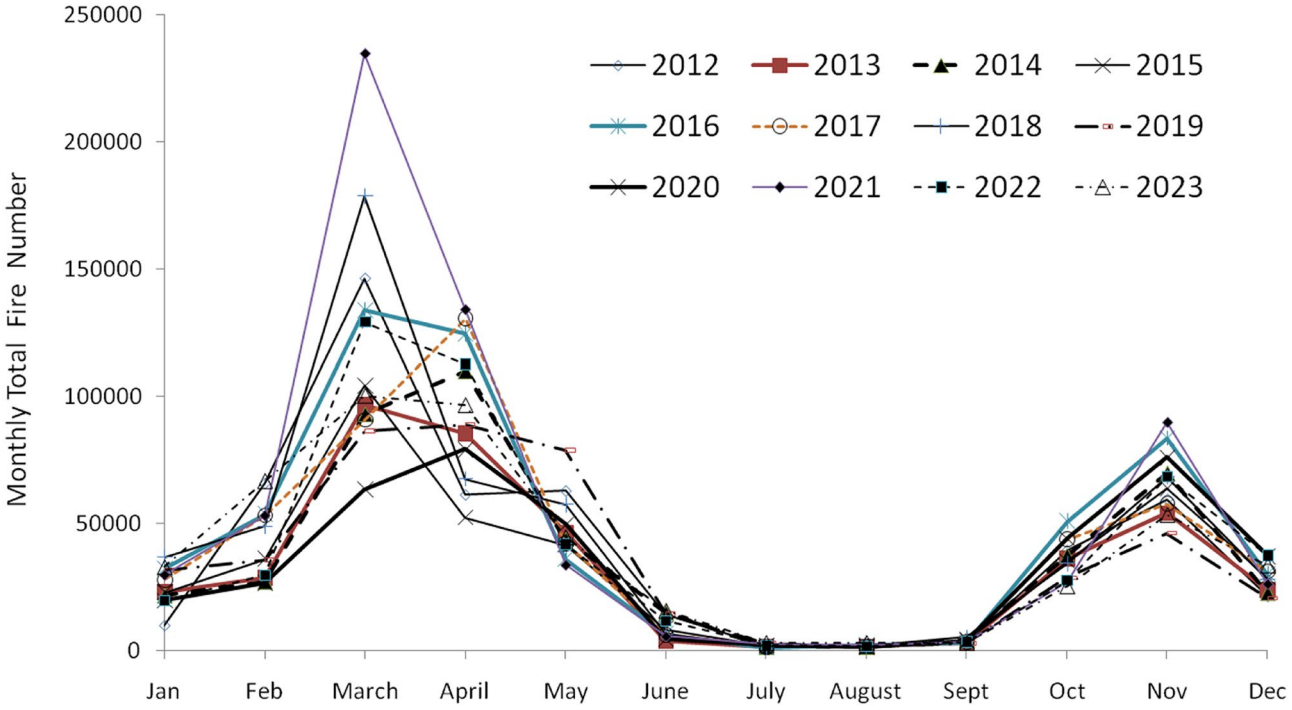

Fig. 1. Variation in monthly total fire count over Indian landmass during 2012 to 2023.

peaking in November and declining thereafter. The fire counts at winter peaks were much lower than summer peaks always, underlining the dominance of summer as the most intense season of fires. Yearly total fire count in 2019 and 2020 were found to have declined to near 2014 and 2015 numbers, possibly reflecting the effect of COVID related slowdown on anthropogenic activities linked to fires.

As per the observed historical fire activity in India during 2012–2023 (Fig. 1), noticeable increase in fires was observed from February onwards consistently every year, corroborating the findings of Global Forest Watch for India as a whole[66] and Indian Institute of Remote Sensing (IIRS) for one of the most wildfire-affected states in India, Uttarakhand. Global Forest Watch reported that peak fire season typically began in mid-February in 2024 based on wildfire data extracted from VIIRS. As per IIRS, who used wildfire data extracted from one of the sensors used by NASA-FIRMS to come to a conclusion, forest fire season in Uttarakhand starts from mid-February, characterized by onset of dry weather and increasing presence of drying vegetation as fuel for fire due

to rising temperature which persists up to mid-June[67]. Considering the remarkable escalation in number of fires from March onwards every year in India, as found in this study (Fig. 1), the 12-month cycle of March–February was chosen as the Indian 'Fire Year' or 'Fire Season' for presenting inter-annual variability in fire activity.

The yearly (fire-year) number of fires ranged from 492,282 (2013–14) to 731,154 (2021–22). The next two most populated years in terms of yearly fire counts were 2016–17 (675,740) and 2018–19 (650,765). The yearly total fire counts, found to be fluctuating during 2012–2023, had a growth rate of 6022 per year (excluding COVID years of 2020–21 and 2021–22) as per Ordinary Least Square (OLS) method with a R^2 value of 0.076 which was found to be statistically non-significant at 5% level (p value = 0.4381) (Fig. 2). When COVID years were included, fire count growth rate increased to 7217 per year with a R^2 value of 0.12, which was also statistically non-significant at 5% level (p value = 0.2685) (Fig. 3). Sen's slope, a non-parametric method used to study linear relationships which is not affected by outliers in the datasets[62], is shown as an alternative trend along with OLS trend. Cluster analysis of all the years under study, each represented by monthly total fire count in respective year (n = 12), revealed that each member year in the pairs of 2017 and 2023, 2016 and 2022, 2013 and 2014 and 2012 and 2018 were statistically similar to each other (Fig. 4).

FRP of individual fires fluctuated within a range of near-zero to 1378.6 MW. The histogram of fire counts falling under various FRP ranges during 2021–2023 represents a positively skewed distribution, reflecting low number of fires beyond the FRP of 500 MW (Fig. 5). The observed difference in individual FRPs is expected due to the variability in amount of biomass burnt, combustion efficiency, biomass composition and moisture content in biomass[68]. The OLS trend of median FRPs per fire (MW) over the study period (excluding COVID years of 2020 and 2021) was slightly negative (− 0.027 MW per year) with a statistically significant R^2 value of 0.608 at 5% level (p value = 0.0078) (Fig. 6), indicating negligible but statistically significant trend of reduction in median FRP per fire during study period. When COVID years were included, the decreasing trend of median FRP per fire was observed to be − 0.020 per year with a R^2 value of 0.411, which was also statistically significant at 5% level (p value = 0.0247) (Fig. 7). Sen's slope is also depicted with the OLS trends.

The annual (fire-year) sum of FRPs ranged from 3,140,642 in 2023–24 to 4,672,833 MW in 2021–22. The OLS trend of annual sum FRPs (MW) over the study period (excluding COVID years of 2020 and 2021) was 1039 MW per year with a statistically non-significant R^2 value of 0.00017 at 5% level (p value = 0.9717) (Fig. 8). The yearly sum FRPs registered an increasing trend from 2012-13 fire year onwards with a rate of 25,534 MW per year when all years under study were considered (Fig. 9). This linear increasing OLS trend was statistically non-significant with a R^2 value of 0.042 (p value = 0.5204). Sen's slope is also depicted with the OLS trends.

There existed a highly significant linear relationship between annual total fire count and annual sum FRPs with a statistically significant R^2, both when COVID years were excluded ($R^2 = 0.839$, p value = 0.002227) or included ($R^2 = 0.89$, p value = 0.001119) in analysis (Fig. 10). This relationship was also reiterated by the concomitant

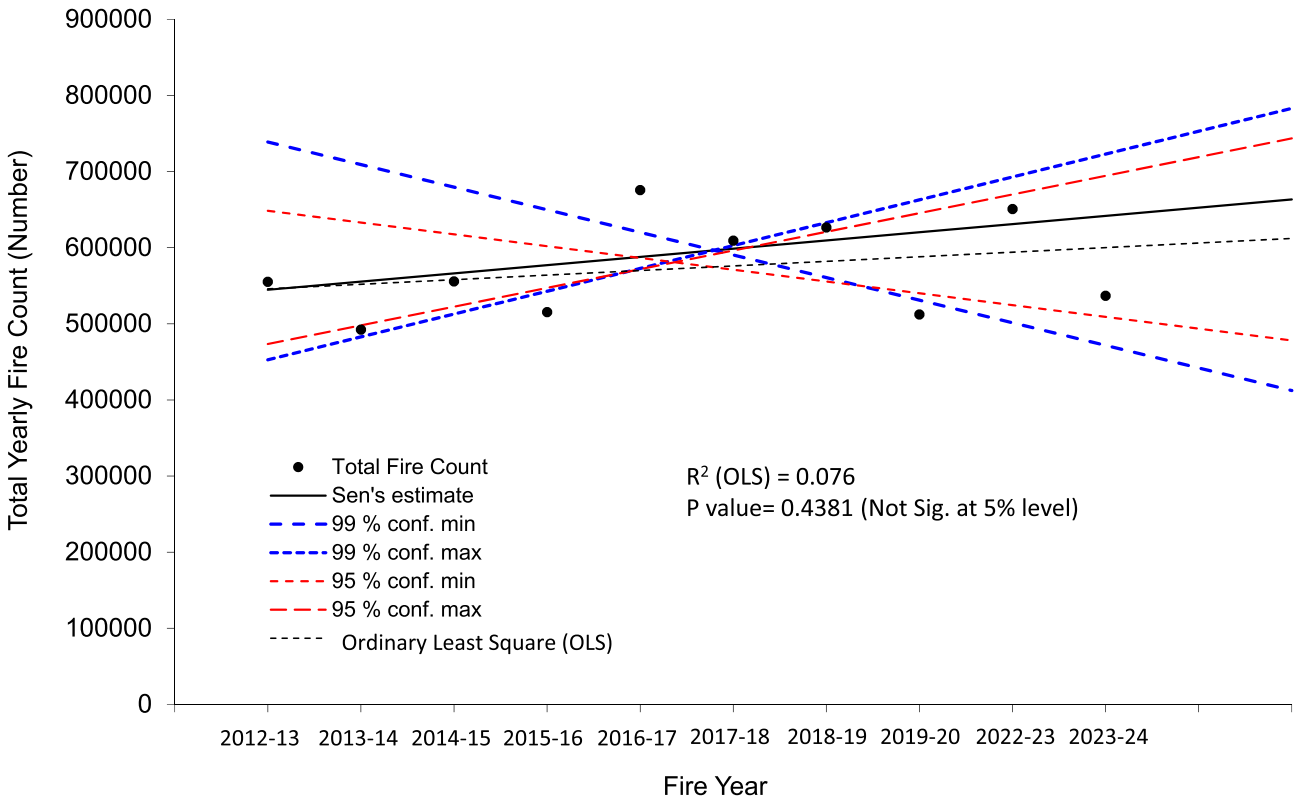

Fig. 2. Yearly trends in annual fire count over 2012–13 to 2023–24 fire-years (without COVID years of ss 2020 and 2021) estimated by OLS and Sen's Method.

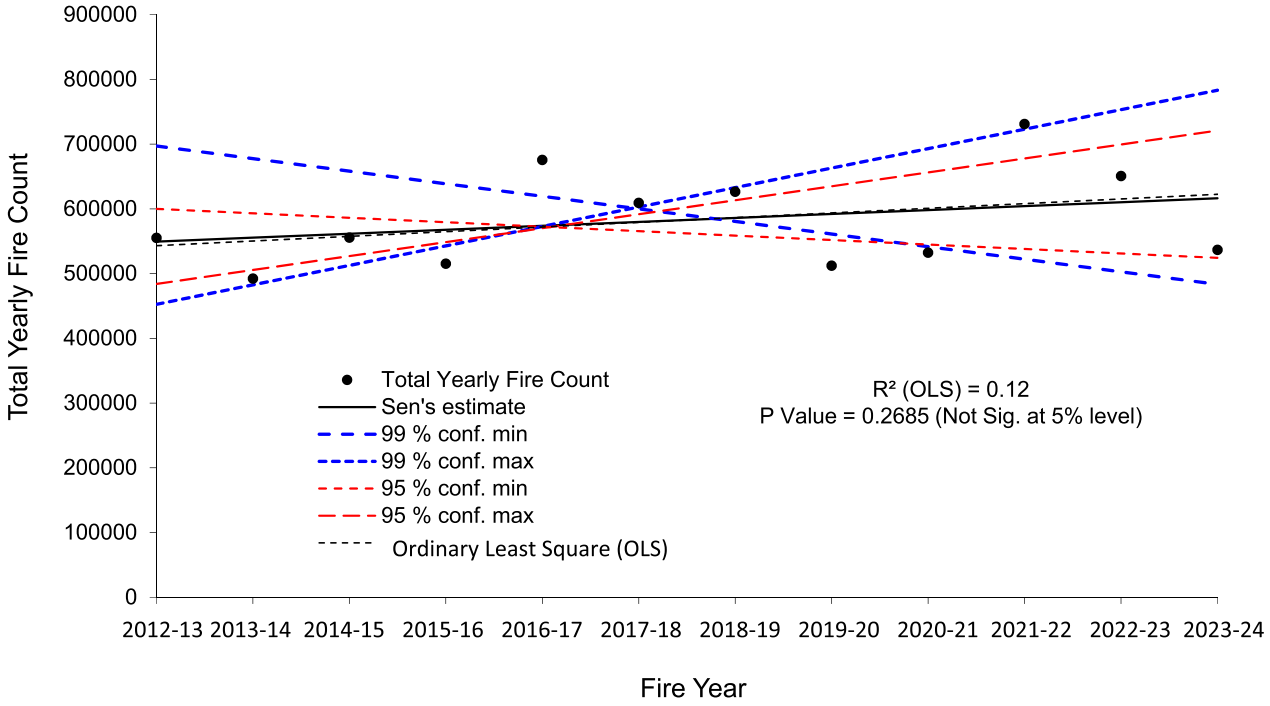

Fig. 3. Yearly trends in annual fire count over 2012–13 to 2023–24 fire-years estimated by OLS and Sen's Method.

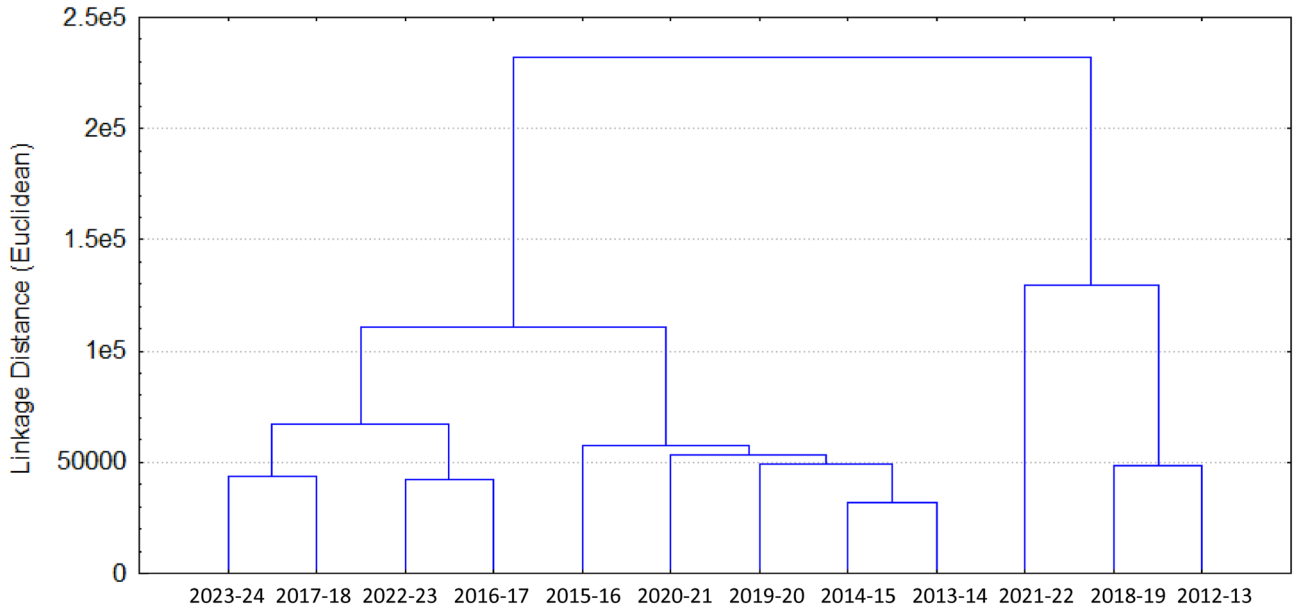

Fig. 4. Dendrogram depicting statistically similar and dissimilar years (fire-years) in terms of monthly total fire counts.

variations in fire count with respective FRPs over the study period (Fig. 11). Cluster analysis of study years based on respective monthly total FRPs (n = 12 each year) indicated that the individual years within the pairs of 2017 and 2023, 2014 and 2020, 2016 and 2022, 2012 and 2015 were statistically similar to each other in terms of monthly sum FRPs (Fig. 12). It has been reported by Vadrevu and Lasko[69] that sum of FRPs from VIIRS data was 2.5 times higher than MODIS sum FRP, as number of fires detected by VIIRS was more in number in an agricultural landscape. Li et al.[26] found that MODIS missed an appreciable number of low-intensity fires in Africa, leading to underestimation of daily MODIS FRP by at least 42.8% than VIIRS FRP.

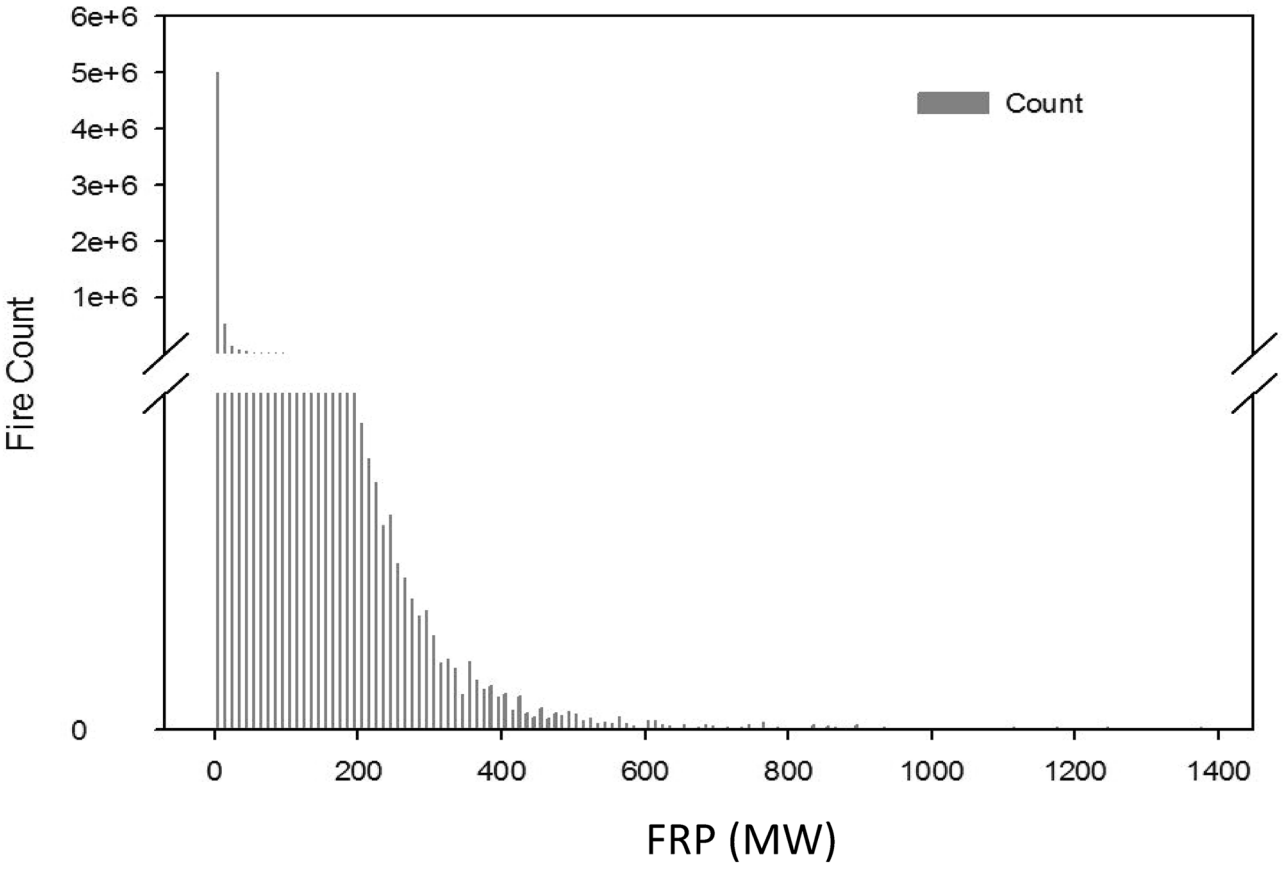

Fig. 5. Histogram of fire counts under various FRP ranges recorded during 2012–2023.

In summers of 2012–2023, fire spots were mainly populated in Central–South–Eastern part of India. The spots covered parts of Odisha, Madhya Pradesh, Chhattisgarh, Telengana, Maharashtra, Andhra Pradesh and Jharkhand, also covering parts of North–Eastern Indian states like Meghalaya, Tripura, Mizoram, lower Assam and Nagaland (Fig. 13). In winter, parts of Northern India in the states of Punjab, Haryana and Uttar Pradesh were mostly affected, followed by central and southern parts of India that hosted scattered fire spots (Fig. 14). The conspicuous clustering of fire spots in major rice and wheat cultivating regions of India in summer and winter builds up a strong case in favour of residue burning in the respective crop harvesting seasons that coincide with periods of March–May and Oct–Nov in India, respectively. Punjab, Haryana, Bihar, Jharkhand, Andhra Pradesh, Madhya Pradesh, Uttar Pradesh, Tamil Nadu, Rajasthan, Maharashtra and Gujarat are the major winter-wheat growing states in India[70]. For winter wheat, stubbles are removed in summer (March–April–May) and put on fire, resulting in a good number of summer fires. The states of Odisha, Andhra and Karnataka, Kerala, West Bengal, Uttar Pradesh, Bihar are known to cultivate summer rice that is harvested around March–April–May[71], indicating to the possibility of paddy stubble burning around this time. Apart from CRB, the prominent numbers of summer forest fire events reported by FSI in India also are expected to substantially contribute to the number of fire spots detected by VIIRS in March–April–May. Some fire clusters overlapped with forested regions of India, predominantly dry/moist deciduous and tropical semi-evergreen types[72] in Madhya Pradesh, Chhattisgarh, Jharkhand, Odisha, Maharashtra, Karnataka, Kerala, Manipur, Meghalaya, Tripura, Mizoram, Nagaland[73,74], indicating occurrence of forest and wildfires. Bahuguna and Upadhyay[75] reported that about 50% of forest fires of India occurred in NE region and95% of them originated from shifting cultivation. During January 2001 to April 2014, around 143,761 forest fire incidents were detected in NER[76]. Also, month-wise fire incidences in NER was maximum in April in Arunachal Pradesh, Assam and Tripura and the minimum in February in all other states, except in Tripura with no fire. States of Nagaland, Manipur, Meghalaya and Mizoram experienced highest number of fires in March. Overall, the decreasing order of fire incidences was: March (54%) > April (43%) > February (3%) in 2014. In NER, evergreen/semi-evergreen forest had highest susceptibility to fire followed by deciduous forests while alpine forests had least vulnerability. Manmade forest fire caused by shifting cultivation is reported to be one of the primary causes of fire incidences in NER. The fire-prone forest areas in India can be traced from the Van Agni Geoportal of FSI[77] which shows extensive coverage of high, very high and extreme fire prone zones in NE India especially in states of Tripura, Meghalaya, Manipur, Nagaland and Mizoram. Further, high to extreme fire-prone zones are also located in several patches in states of Odisha, Telengana and Chhattisgarh which are all observed to be affected by fires during 2012–2021.

Fire spot density in the worst affected summer and winter months of 2022 (March and November) and 2023 (April and November) were analyzed and mapped in 20 km × 20 km grids over Indian landmass vis a vis the

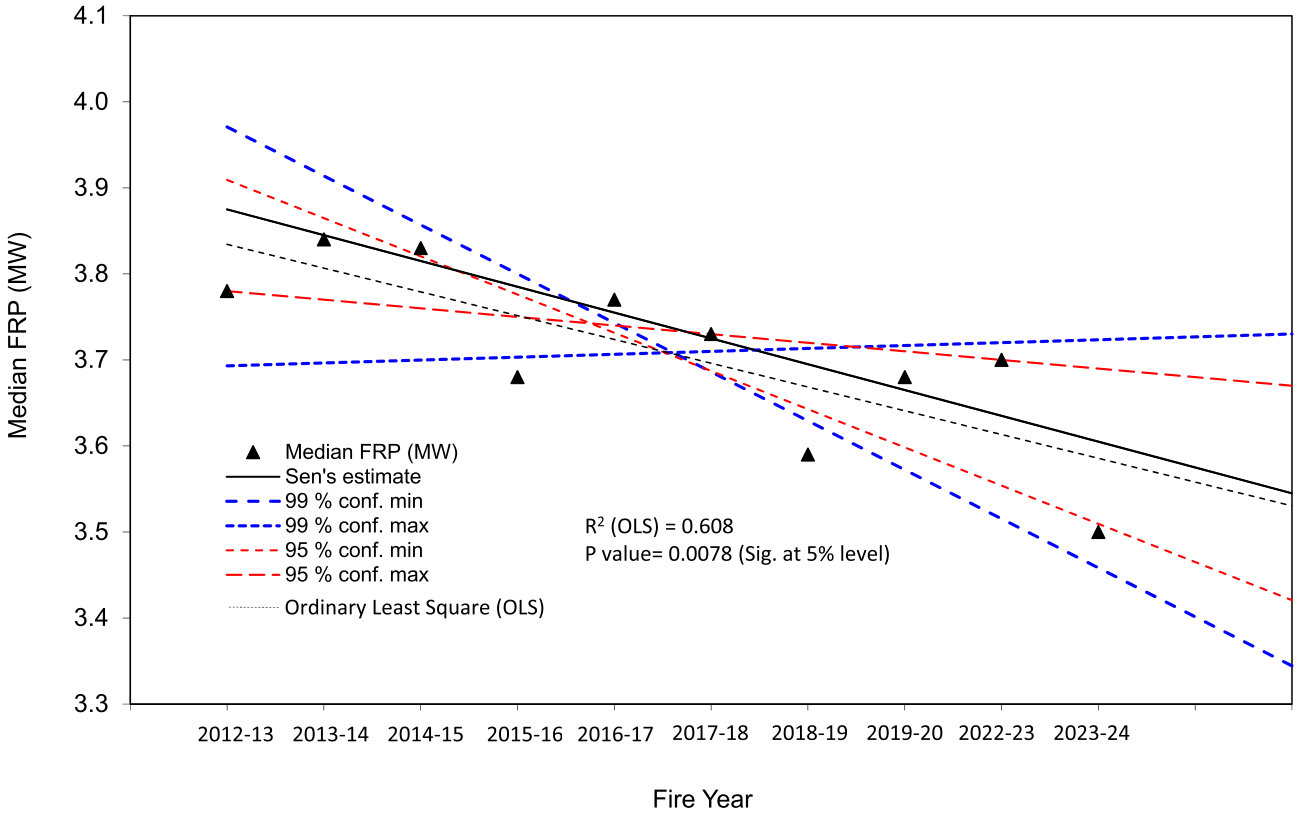

Fig. 6. Yearly trends in median FRP over 2012–13 to 2023–24 fire-years (without COVID years of 2020 and 2021) estimated by OLS and Sen's Method.

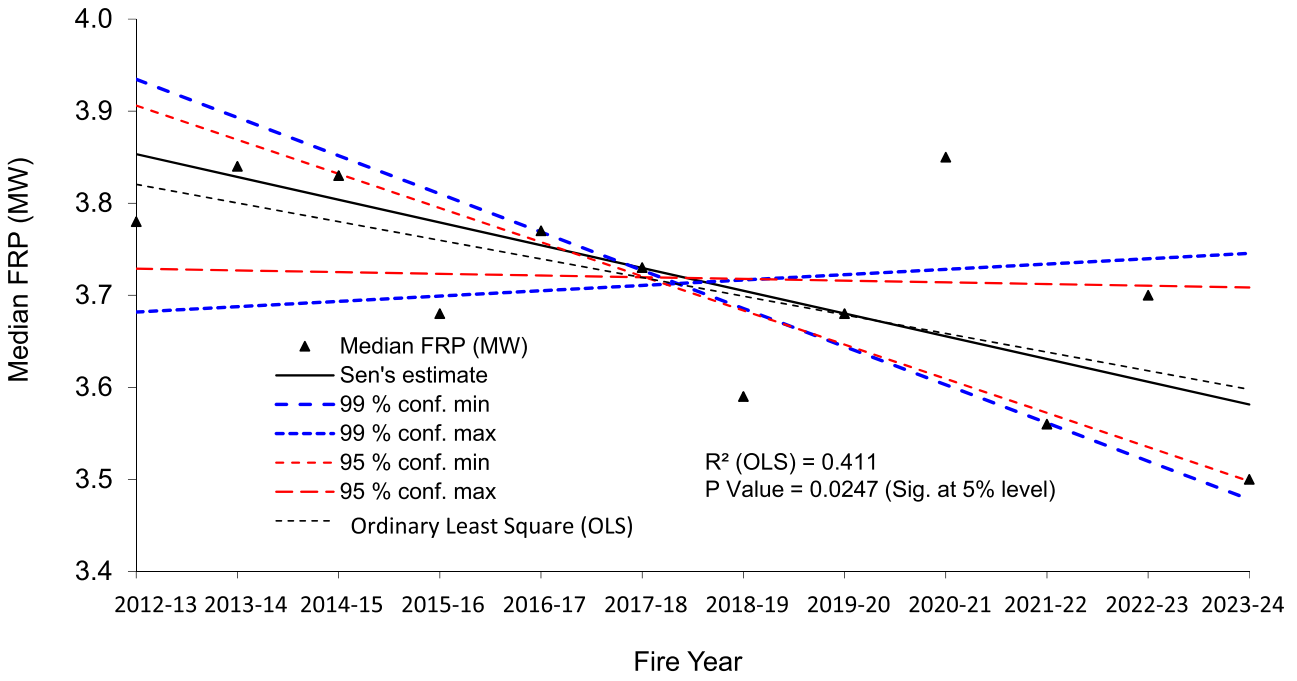

Fig. 7. Yearly trends in median FRP over 2012–13 to 2023–24 fire-years estimated by OLS and Sen's Method.

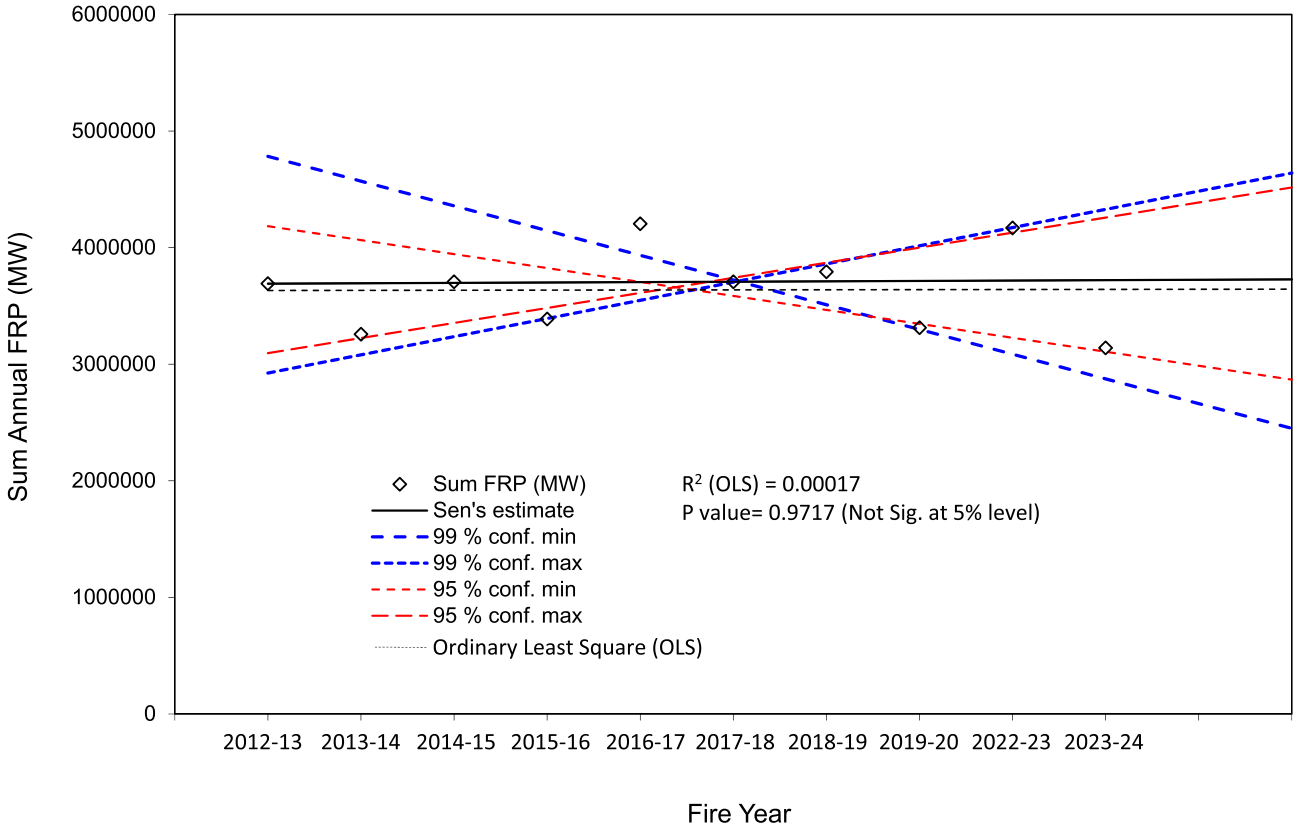

Fig. 8. Yearly trends in annual sum FRP over 2012–13 to 2023–24 fire-years (without COVID years of 2020 and 2021) estimated by OLS and Sen's Method.

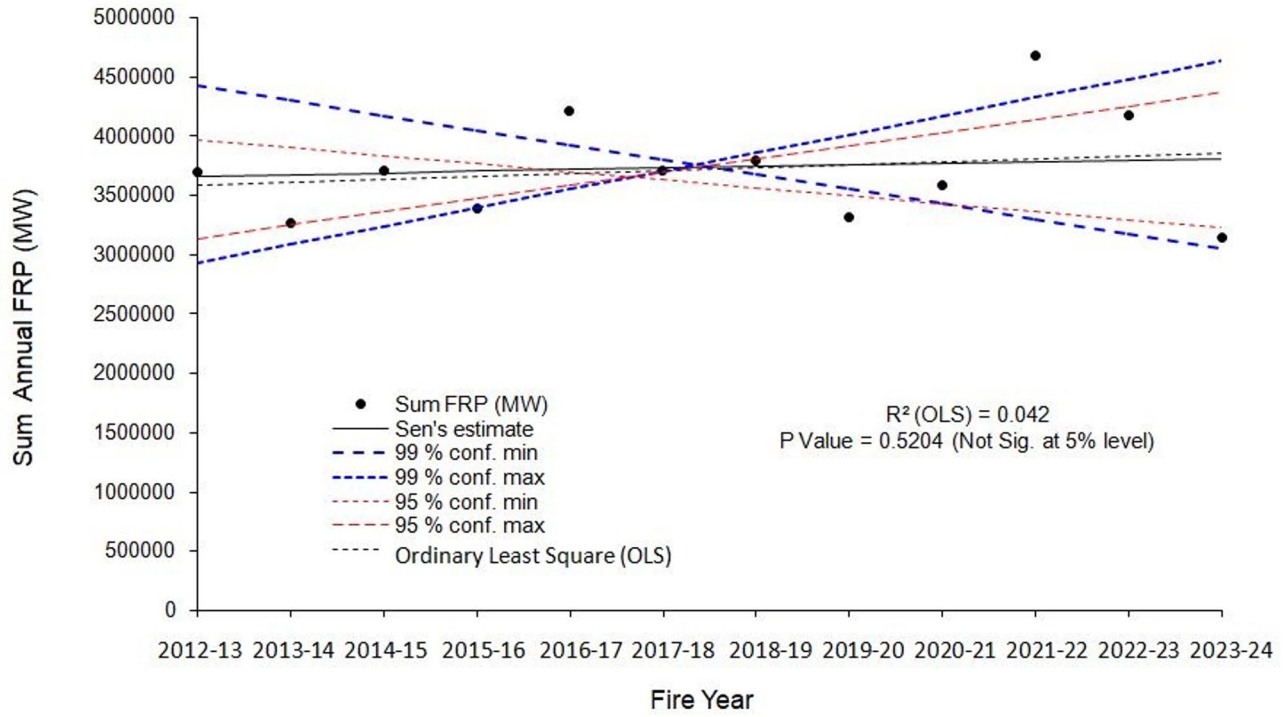

Fig. 9. Yearly trends in annual sum FRP over 2012–13 to 2023–24 fire-years estimated by OLS and Sen's Method.

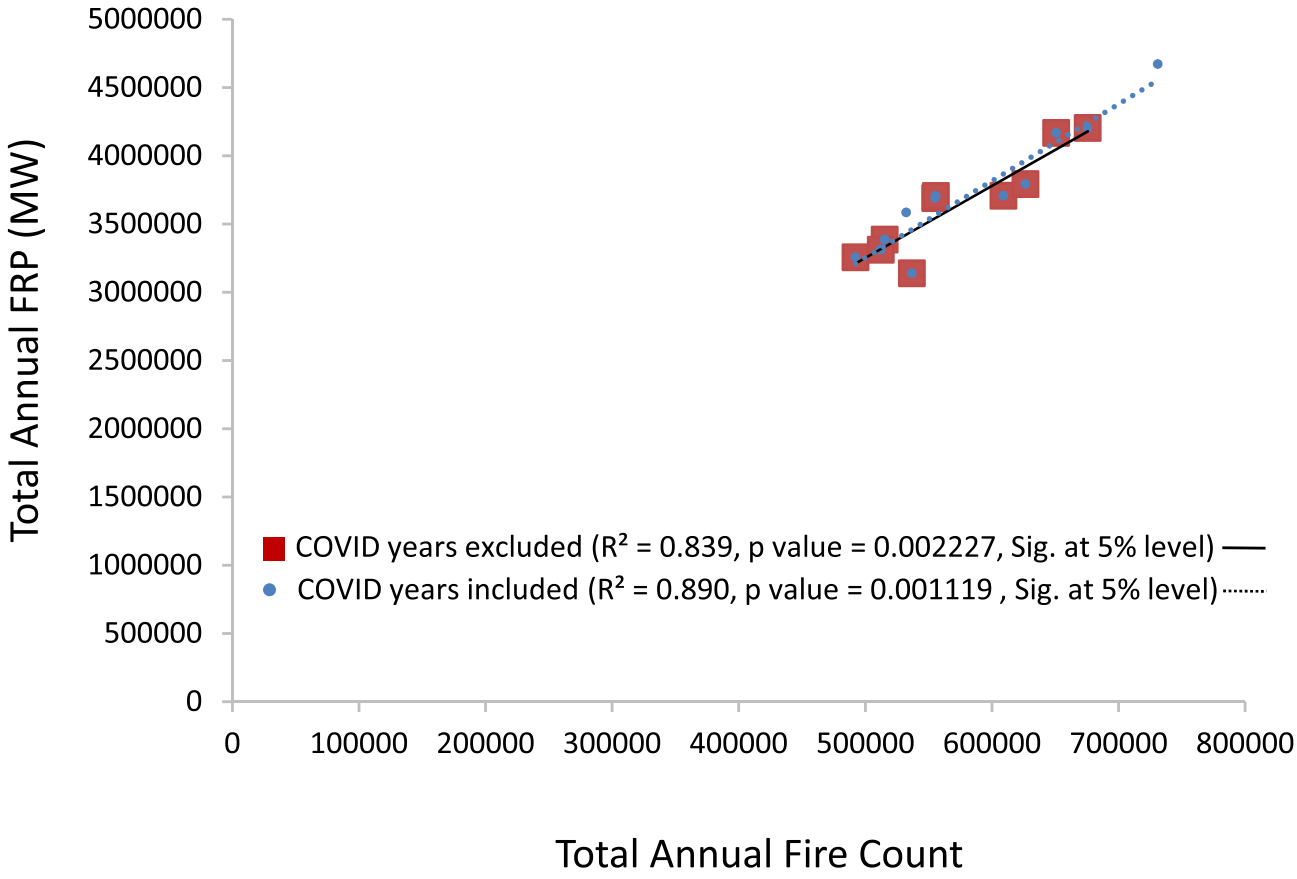

Fig. 10. Linear variation in sum annual FRPs with total annual fire counts over 2012–13 to 2023–24 (with and without inclusion of COVID years).

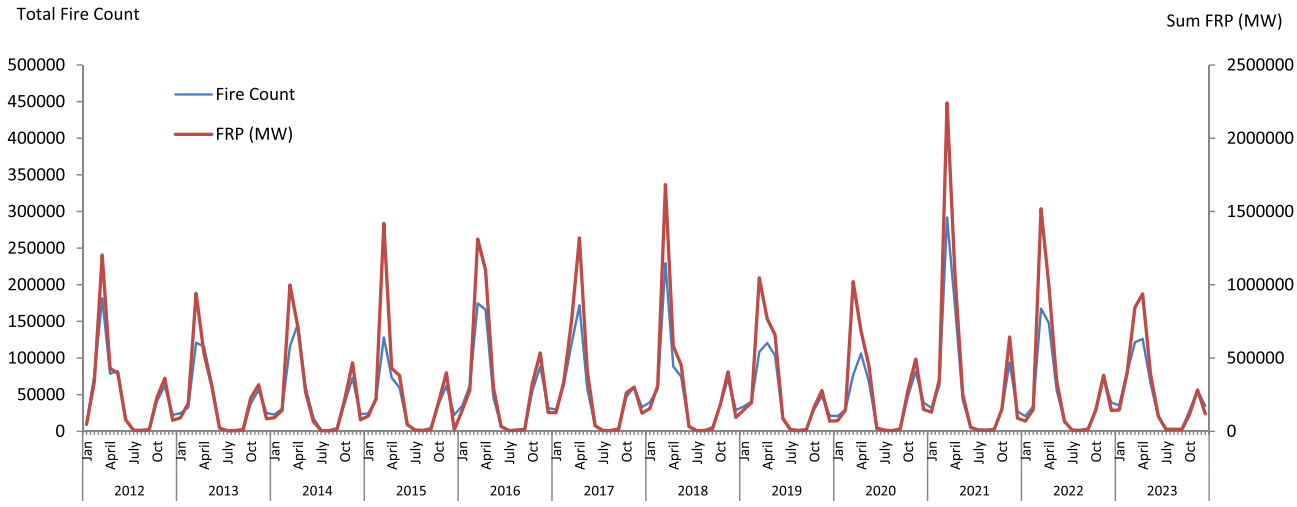

Fig. 11. Concomitant fluctuations in monthly sum FRPs with monthly fire counts over 2012–2023.

number of fire spots detected in the grids. The grids can also be designated as fire hot spots of various degrees in terms of fire counts. The locations of cities with > 1 lakh (0.1 million) population were overlaid on Indian landmass to visualize the proximity or overlapping of cities with various classes of fire hot spots hosting specific numbers of fires (Figs. 15, 16, 17 and 18). It is observed that many of summer and winter fire hot spots (400 km^2 area) indeed hosted some well-known and populated cities. In the winter (November) of 2022 and 2023, well-known cities like Amritsar, Abohar, Jalandhar, Ludhiana, Patiala and Pathankot in state of Punjab were found to be within 400 km^2 hot-spot grids (100–750). Further away, Chandigarh, NCR of Delhi, and cities like Hisar,

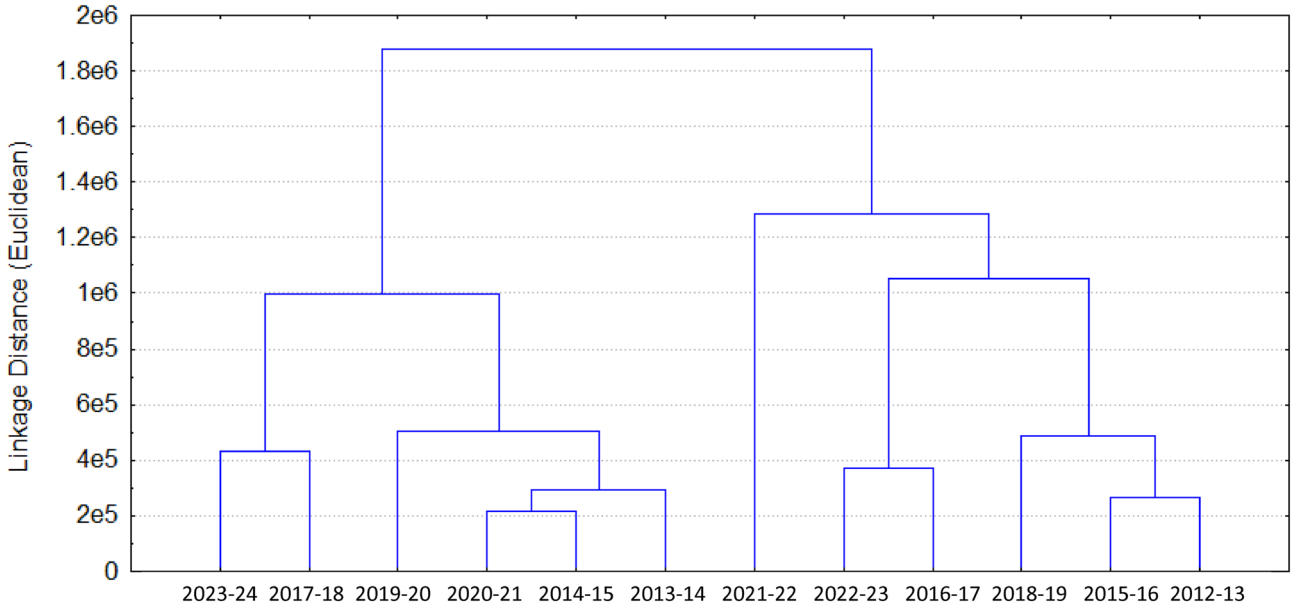

Fig. 12. Dendrogram depicting pairs of statistically similar and dissimilar years (fire-years) in terms of sum FRPs.

Sonepath, Karnal, Faridabad and Gurgaon in state of Haryana, Nizamabad and Kakinada in Telengana etc. were also located in hot spot grids in either 2022–23 or 2023–24 and wildfire impacts may also be expected at some of these urban centres. Notably, the said impacts were not measured or assessed but only perceived based on geographical proximity. Several other cities in states of Uttar Pradesh (Ghaziabad, Muzaffarnagar, Saharanpur, Bareilly, Hapur, Bulandshahar, Gorakhpur, Varanasi, Rampur); Madhya Pradesh (Jabalpur, Bhopal, Gwalior); West Bengal (Kulti, Durgapur, Asansol); Dibrugarh and Dispur in Assam; Imphal in Manipur etc. are also located within some prominent fire hot spots either in 2022–23 or in 2023–24 winter season (Fig. 15-16). There are more number of cities and small towns positioned in an around the wintertime wildfire hot spots that are not separately discussed here.

On the other hand, some of the well-known and populated cities located near summer fire hot spots were Delhi; Karnal, Sonepat and Panipat in Haryana; Gorakhpur, Muzaffarnagar, Meerut in Uttar Pradesh; Mumbai, Thane, Pune, Nasik and Nagpur in Maharashtra; Jabalpur, Ratlam, Gwalior, Sagar, Sannai, Bhopal, Sagar, Vidisha etc. in Madhya Pradesh; Hyderabad, Secunderabad, Nellore, Cuddapah etc. in Andhra Pradesh; Chennai and Coimbatore in Tamil Nadu; Trichur in Kerala; Asansol and Durgapur in West Bengal; Dhanbad in Jharkhand; Cuttack and Bhubaneswar in Odisha; Shillong in Meghalaya; Dibrugarh, Guwahati in Assam; Aizwal in Mizoram and Imphal in Manipur etc. There are many other towns and small cities positioned near summertime wildfire hot spots that are not separately discussed here (Fig. 17-18). The proximity of many of these populated towns and cities to the fire hot spots either in 2022 or in 2023 summer season underlines the potential scope of having wildfire-related impacts on environment. FSI's Van Agni portal provides interactive viewing of forest fires and fire clusters vis a vis forest administrative boundaries, forest type and cover, fire prone forest area etc. in which a user can visualise NRT forest fires detected by MODIS & VIIRS during last three days. The portal also thematically depicts forest fire risk zones based on last several years' data. The wildfire hot-spot maps provided in this paper demonstrate seasonally classified grids based on number of wildfires that would assist in easy visualization and comparison of highly affected, moderately affected and non-affected grids in terms of various ranges of fire numbers. Importantly, position of populated cities or groups of cities falling within specific grids can be visualized that could possibly indicate the extent of intervention needed for addressing potential short-term local impacts of wildfires in these towns and cities.

Studies indicate that wildfires can have measurable and statistically significant effect on urban centres[78]. In US, a large number of houses were found to have been built since 1990 within or near natural vegetation, in areas designated as the Wildland-Urban Interface (WUI), and by 2017, about one in three houses and one in ten hectares of land were located in the WUI. This observed growth in WUI in US is expected to aggravate wildfire-related problems on humans and their livelihood in future[79]. In California during 1985–2013, interface WUI areas hosted about 50% of buildings that were destroyed in wildfire, whereas intermix WUI had about 32% of the destroyed buildings[80]. Chen et al.[81] have reported that expanding wildfires and human settlements have put higher number of people and infrastructure within the realm of WUI areas under risk. They estimated that 7.07% (12.54%) of WUI areas, hosting about 4.47 million (10.11 million) people, are coming within a 2400 m (4800 m) buffer zone of wildfire threat. Countries like United States, Brazil, China, India and Australia have highest share in WUI areas. In case of large wildfires, air parcels can carry smoke to large distances in short time and air quality in urban centers near fire clusters may get affected substantially, as have been reported from India[82,83], Australia[84], Southeast China[85], apart from perturbations in local and regional climate and radiation

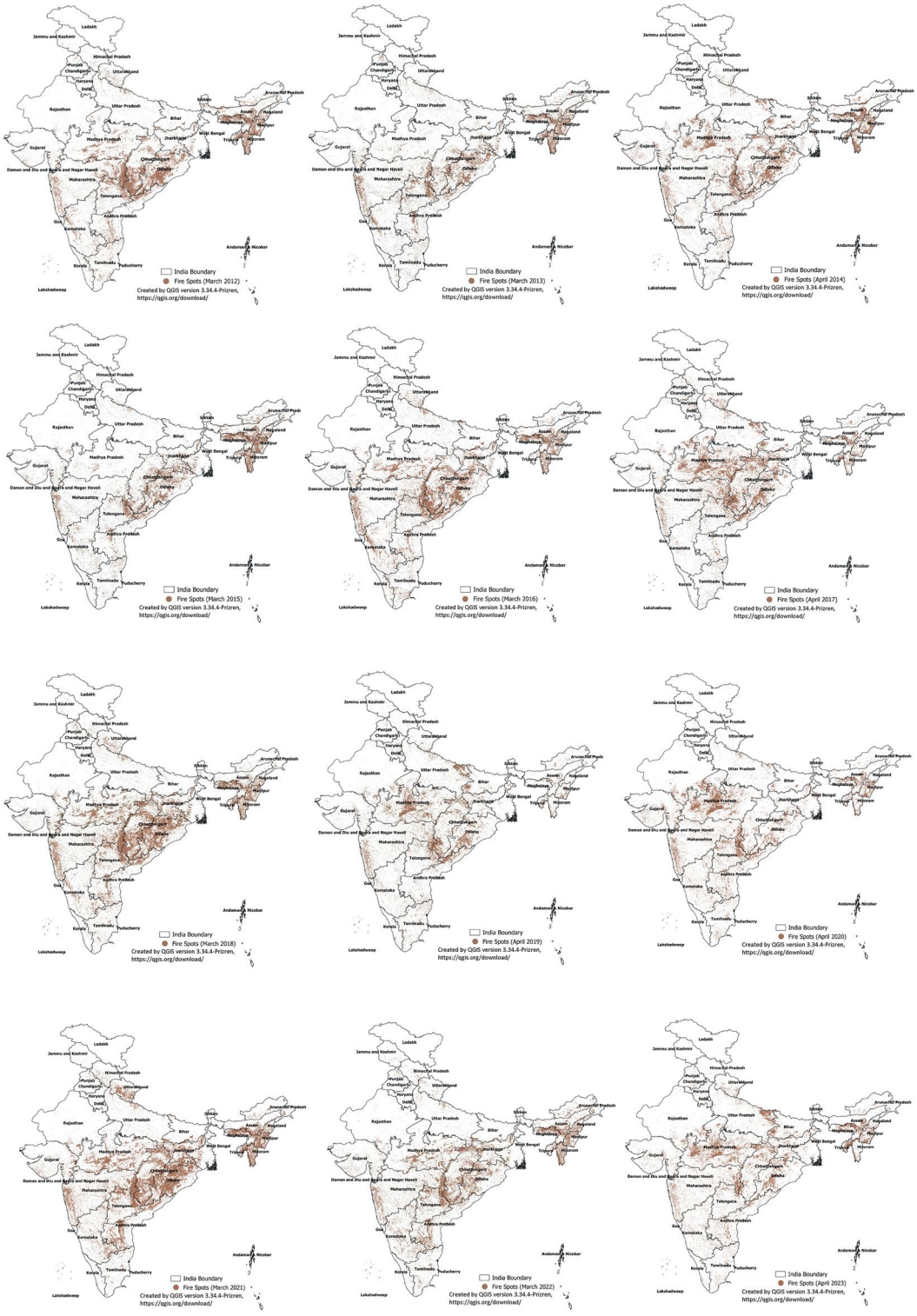

Fig. 13. Indian landmass dotted with fire spots in the months of maximum occurrence (March or April) in summer in each year during 2012 to 2023 (Maps created by QGIS version 3.34.4-Prizren, https://qgis.org/download/).

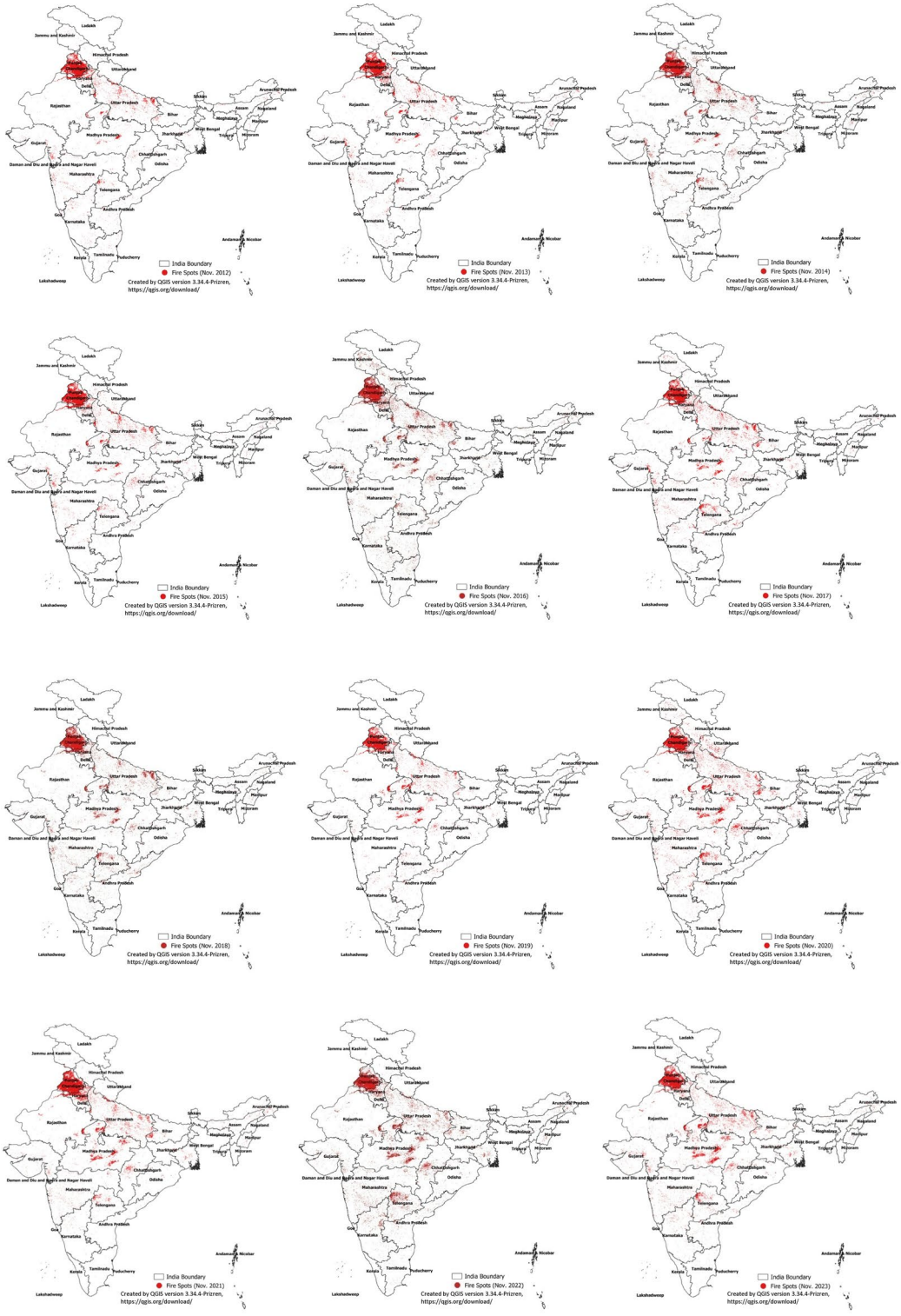

Fig. 14. Indian landmass dotted with fire spots in months of maximum occurrence (November) in winter in each year during 2012 to 2023 (Maps created by QGIS version 3.34.4-Prizren, https://qgis.org/download/).

budgets in a few aggravated cases[86]. Fire hot spot identification by density mapping technique, as used in this paper, has been deployed by Tonini et al.[87] in Portugal also that facilitated easy visualization of the fire hot spots.

Conclusion

Analysis of fire spots and their FRPs during 2012–2023 could answer some of the questions posed at the onset of the study. There are yearly fluctuations in wildfire number and total annual FRP and evidences on slight increase

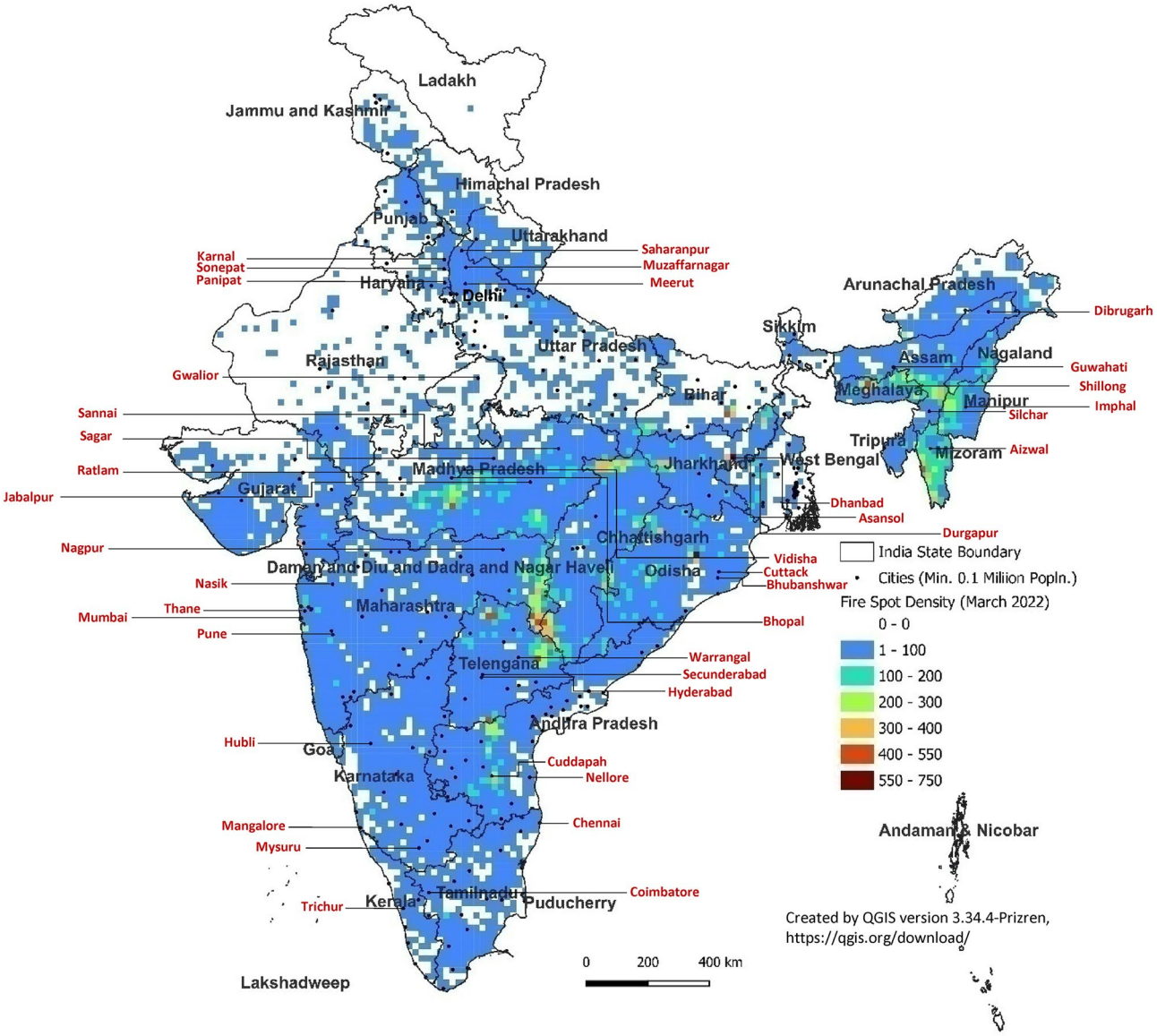

Fig. 15. Fire hot spots relative to locations of cities with > 0.1 million population in 20 km × 20 km grids over India in the month of maximum detected fire number (Nov.) in winter 2022 (Maps created by QGIS version 3.34.4-Prizren, https://qgis.org/download/).

in annual fire counts and sum FRPs over 2012 to 2023. But, these trends were found statistically insignificant. But nevertheless, the hint of increase should be viewed with caution due to potentially grave impacts of repeated wildfires on environmental sustainability. There is a clear seasonality in fire incidents, summer being the worst affected season. Winter fires are much lesser in number and mostly centred around specific areas in a few North Indian states viz. Punjab and Haryana followed by Uttar Pradesh. Existence of some populated cities (> 0.1 million population) within fire hot spot grids is apparent, implying the scope of potential impacts of fires on urban life, and air environment. It may be noted that these perceived impacts on nearby urban centres are inferred from proximity of cities to wildfire clusters and not from direct measurement of exposure or effects.

Studies on positional changes in fire-prone areas over the last decade and likely future scenarios, likelihood of having high-intensity fires in the changing climate, estimation of burnt-areas, mapping of vulnerable WUIs and innovations in fire-resilient living under local conditions are potentially important to know in India through future studies, which were not covered under this study. Other potential additions to this work in future could be to identify and clearly differentiate between fire types and assess the extent of burnt areas, keeping in view the challenge of doing so in a large study domain i.e. the entire Indian landmass. Proactive participation of local inhabitants along with interventions by state administrations are urgently needed to streamline and promote sustainable eco-practices to minimize incidence of natural fires, inadvertently caused fires and arson in India.

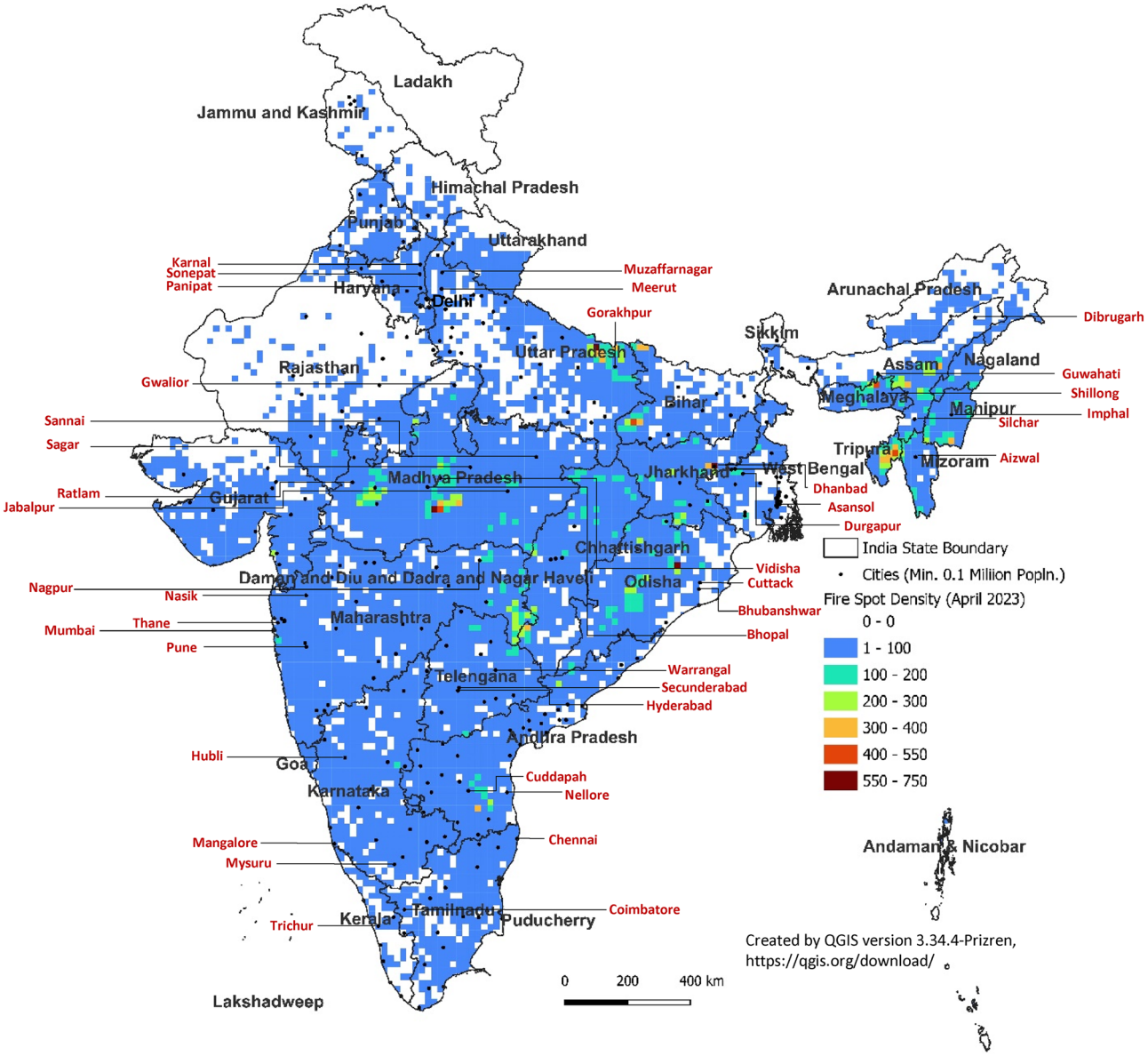

Fig. 16. Fire hot spots relative to locations of cities with > 0.1 million population in 20 km × 20 km grids over India in the month of maximum detected fire number (Nov.) in winter 2023 (Maps created by QGIS version 3.34.4-Prizren, https://qgis.org/download/).

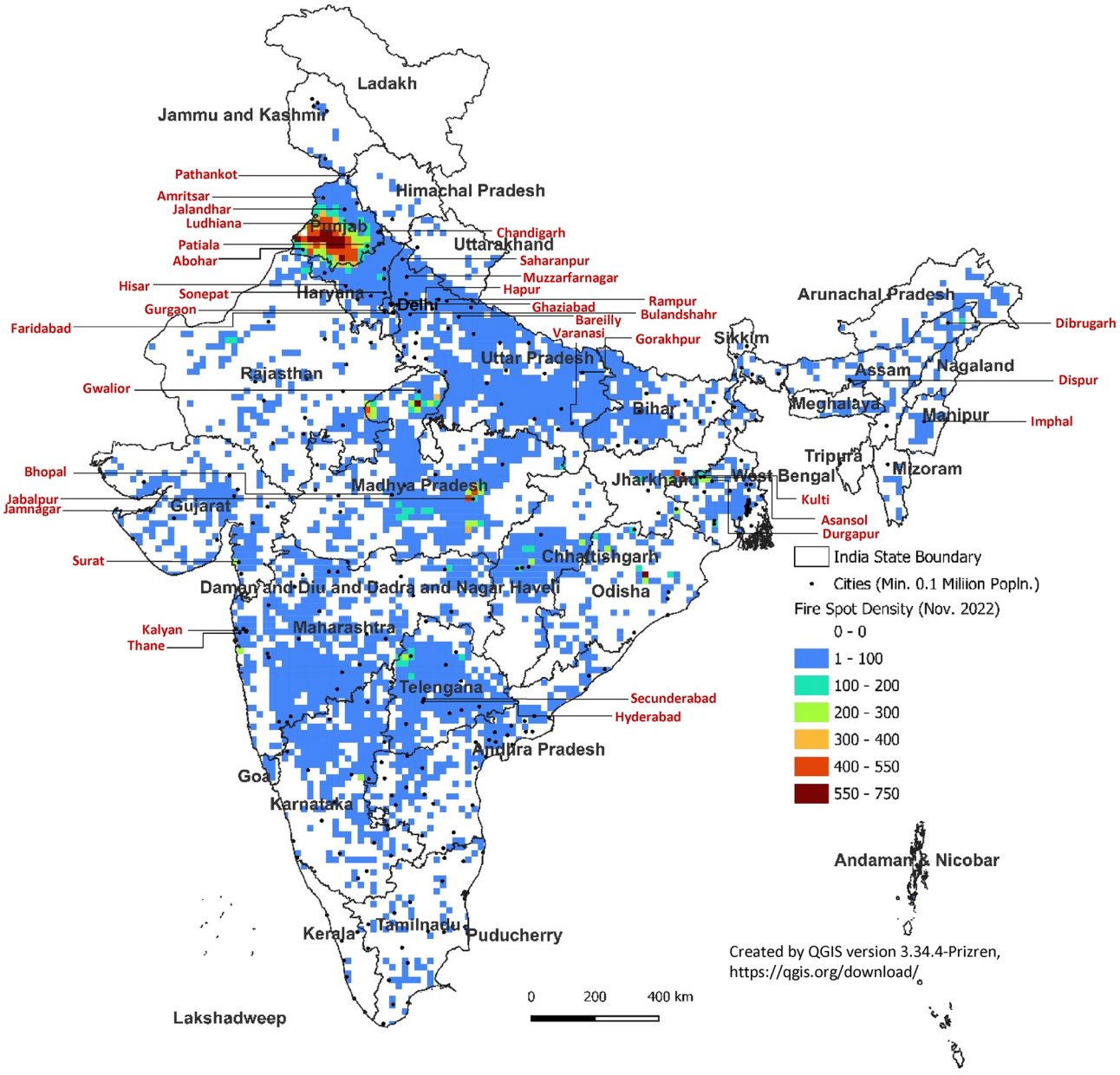

Fig. 17. Fire hot spots relative to locations of cities with > 0.1 million population in 20 km × 20 km grids over India in the month of maximum detected fire number (March) in summer 2022 (Maps created by QGIS version 3.34.4-Prizren, https://qgis.org/download/).

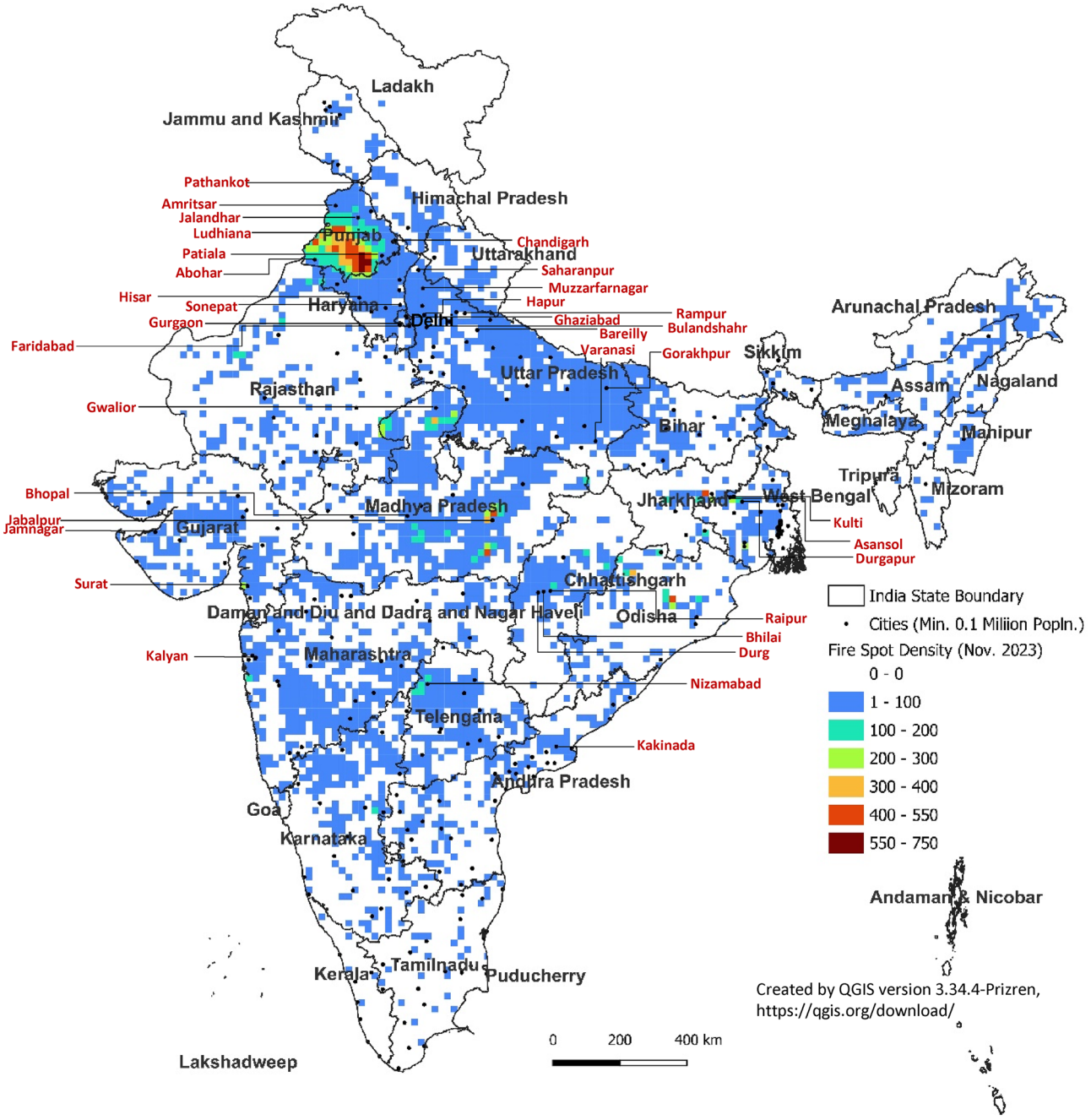

Fig. 18. Fire hot spots relative to locations of cities with > 0.1 million population in 20 km × 20 km grids over India in the month of maximum detected fire number (April) in summer 2023 (Maps created by QGIS version 3.34.4-Prizren, https://qgis.org/download/).

Data availability

The satellite datasets extracted for the current study are open-access data and hence, are available to everyone for free downloading.

Received: 3 August 2024; Accepted: 8 July 2025
Published online: 26 July 2025

References

1. Crutzen, P. J. & Andreae, M. O. Biomass burning in the tropics: Impact on atmospheric chemistry and biogeochemical cycles. *Science* **250**(4988), 1669–1678. https://doi.org/10.1126/science.250.4988.1669 (1990).
2. Jain, N., Bhatia, A. & Pathak, H. Emission of air pollutants from crop residue burning in India. *Aerosol Air Qual. Res.* **14**, 422–430. https://doi.org/10.4209/aaqr.2013.01.0031 (2014).

3. Csiszar, I. et al. Active fires from the Suomi NPP visible infrared imaging radiometer suite: Product status and first evaluation results. *J. Geophys. Res. Atmos.* **119**(2), 2013JD020453. https://doi.org/10.1002/2013JD020453 (2014).
4. Hao, W. M. & Liu, M. H. Spatial and temporal distribution of tropical biomass burning. *Glob. Biogeochem. Cycles* **8**, 495–503. https://doi.org/10.1029/94GB02086 (1994).
5. Cunningham, C. X., Williamson, G. J. & Bowman, D. M. J. S. Increasing frequency and intensity of the most extreme wildfires on Earth. *Nat. Ecol. Evol.* **8**, 1420–1425. https://doi.org/10.1038/s41559-024-02452-2 (2024).
6. Jones, M. W. et al. State of wildfires 2023–2024. *Earth Syst. Sci. Data* **16**, 3601–3685. https://doi.org/10.5194/essd-16-3601-2024 (2024).
7. UNEP (United Nations Environment Programme). *Global Peatlands Assessment*: *The State of the World's Peatlands*, *Nairobi*, *Kenya*, accessed 12 September 2024; https://www.unep.org/resources/global-peatlands-assessment-2022 (2022).
8. Ponomarev, E. I., Zabrodin, A. N., Shvetsov, E. G. & Ponomareva, T. V. Wildfire intensity and fire emissions in Siberia. *Fire* **6**, 246. https://doi.org/10.3390/fire6070246 (2023).
9. Ell, K. Moody's *Analytics research, weekly market outlook*, accessed 14 September 2020; https://www.moodysanalytics.com/-/media/article/2020/weekly-market-outlook-overvalued-equities-increase-corporate-credits-downside-risk.pdf (2020).
10. Corpuz, J. C. G. Heatwaves, wildfires and global warming: A call to public health action. *J. Public Health* **46**(2), e326–e327. https://doi.org/10.1093/pubmed/fdad242 (2024).
11. Streets, D. G., Yarber, K. F., Woo, J. H. & Carmichael, G. R. An inventory of gaseous and primary aerosol emissions in Asia in the year 2000. *J. Geophys. Res.* **108**, 8809–8823. https://doi.org/10.1029/2002JD003093 (2003).
12. Zhang, L., Liu, Y. & Lu, H. Contributions of open crop straw burning emissions to $PM_{2.5}$ concentrations in China. *Environ. Res. Lett.* **11**(1), 014014. https://doi.org/10.1088/1748-9326/11/1/014014 (2016).
13. Yadav, I. C. & Devi, N. L. Biomass burning, regional air quality, and climate change. In *Earth Systems and Environmental Sciences. Edition: Encyclopedia of Environmental Health* 2nd edn (ed Nriagu, J. J.) (Elsevier, 2018). https://doi.org/10.1016/B978-0-12-409548-9.11022-X.
14. Ravindra, K., Singh, T. & Mor, S. Emissions of air pollutants from primary crop residue burning in India and their mitigation strategies for cleaner emissions. *J. Clean. Prod.* **208**, 261–273. https://doi.org/10.1016/j.jclepro.2018.10.031 (2018).
15. IARI. *Crop Residues Management with Conservation Agriculture: Potential, Constraints and Policy Needs* 7–32 (Indian Agricultural Research Institute, 2012).
16. Vadrevu, K. P., Ellicott, E., Badarinath, K. V. S. & Vermote, E. MODIS derived fire characteristics and aerosol optical depth variations during the agricultural residue burning season, north India. *Environ. Poll.* **159**, 1560–1569. https://doi.org/10.1016/j.envpol.2011.03.001 (2011).
17. Jitendra, S. V. et al. India's burning issues of crop burning takes a new turn. *Down to Earth*, accessed on 7 December 2021; https://www.downtoearth.org.in/coverage/river-of-fire-57924 (2017).
18. Gadde, B., Bonnet, S., Menke, C. & Garivait, S. Air pollutant emissions from rice straw open field burning in India Thailand and the Philippines. *Environ. Poll.* **157**, 1554–1558. https://doi.org/10.1016/j.envpol.2009.01.004 (2009).
19. Forest Survey of India. India State of Forest Report. Forest Survey of India (Ministry of Environment & Forests, 2015).
20. Forest Survey of India. India State of Forest Report. Forest Survey of India (Ministry of Environment & Forests, 2019).
21. Forest Survey of India. Accessed on 9 January 2024; https://fsi.nic.in/forest-fire-activities?pgID=forest-fire-activities.
22. Sahu, L. K. et al. Regional biomass burning trends in India: Analysis of satellite fire data. *J. Earth Syst. Sci.* **124**, 1377–1387. https://doi.org/10.1007/s12040-015-0616-3 (2015).
23. Ahmad, F. & Goparaju, L. Forest fire trend and influence of climate variability in India: A geospatial analysis at national and local scale. *Ekológia* **38**(1), 49–68. https://doi.org/10.2478/eko-2019-0005 (2019).
24. Jain, M., Saxena, P., Sharma, S. & Sonwani, S. Investigation of forest fire activity changes over the central India domain using satellite observations during 2001–2020. *Geo Health* **5**, e2021GH000528. https://doi.org/10.1029/2021GH000528 (2021).
25. Mohanty, A. & Mithal, V. *Managing Forest Fires in a Changing Climate* (Council on Energy, Environment and Water, 2022). https://www.ceew.in/publications/states-vulnerable-to-forest-fire-events-india-and-mitigation-measures.
26. Li, F., Zhang, X. & Kondragunta, S. Biomass burning in Africa: An investigation of fire radiative power missed by MODIS using the 375 m VIIRS active fire product. *Remote Sens.* **12**, 1561. https://doi.org/10.3390/rs12101561 (2020).
27. Lasslop, G. & Kloster, S. Human impact on wildfires varies between regions and with vegetation productivity. *Environ. Res. Lett.* **12**, 115011. https://doi.org/10.1088/1748-9326/aa8c82 (2017).
28. Seitinthang, L. Cropping pattern of north east India: An appraisal. *Am. Res. Thoughts* **1**(1), 488–498 (2014).
29. Banerjee, P. MODIS-FIRMS and ground-truthing-based wildfire likelihood mapping of Sikkim Himalaya using machine learning algorithms. *Nat. Haz.* **110**, 899–935. https://doi.org/10.1007/s11069-021-04973-6 (2021).
30. Shikhov, A. N., Perminova, E. S. & Perminov, S. I. Satellite-based analysis of the spatial patterns of fire and storm-related forest disturbances in the Ural region, Russia. *Nat. Haz.* **97**, 283–308. https://doi.org/10.1007/s11069-019-03642-z (2019).
31. Wooster, M., Roberts, G., Perry, G. L. W. & Kaufman, Y. J. Retrieval of biomass combustion rates and totals from fire radiative power observations: FRP derivation and calibration relationships between biomass consumption and fire radiative energy release. *J. Geophys. Res.-Atmos.* **110**(24), D24311. https://doi.org/10.1029/2005JD006318 (2005).
32. Roy, D. P. & Kumar, S. S. Multi-year MODIS active fire type classification over the Brazilian tropical moist forest biome. *Int. J. Digital Earth* **10**(1), 54–84. https://doi.org/10.1080/17538947.2016.1208686 (2017).
33. Schroeder, W., Csiszar, I., Giglio, L. & Schmidt, C. C. On the use of fire radiative power, area, and temperature estimates to characterize biomass burning via moderate to coarse spatial resolution remote sensing data in the Brazilian Amazon. *J. Geophys. Res.* **115**, D21121. https://doi.org/10.1029/2009JD013769 (2010).
34. Schroeder, W., Oliva, P., Giglio, L. & Csiszar, I. A. The new VIIRS 375m active fire detection data product: Algorithm description and initial assessment. *Remote Sens. Environ.* **143**, 85–96. https://doi.org/10.1016/j.rse.2013.12.008 (2014).
35. Zhang, T., Wooster, M. J. & Xu, W. Approaches for synergistically exploiting VIIRS I- and M-Band data in regional active fire detection and FRP assessment: A demonstration with respect to agricultural residue burning in Eastern China. *Remote Sens. Environ.* **198**, 407–424. https://doi.org/10.1016/j.rse.2017.06.028 (2017).
36. Gurjar, B. R., Ravindra, K. & Nagpure, A. S. Air pollution trends over Indian megacities and their local-to-global implications. *Atmos. Environ.* **142**, 475–495. https://doi.org/10.1016/j.atmosenv.2016.06.030 (2016).
37. Bond, T. C. et al. Bounding the role of black carbon in the climate system: A scientific assessment. *J. Geophys. Res.* **118**, 5380–5552. https://doi.org/10.1002/jgrd.50171 (2013).
38. Srivastava, S. & Senthil Kumar, A. Implications of intense biomass burning over Uttarakhand in April–May 2016. *Nat. Haz.* **101**, 367–383. https://doi.org/10.1007/s11069-020-03877-1 (2020).
39. Santi, P., Cannon, S. & DeGraff, J. Wildfire and landscape change. In *Treatise on Geomorphology* Vol. 13 262–287 (Academic Press, 2013).https://doi.org/10.1016/B978-0-12-818234-5.00017-1.
40. Rengers, F. K. Wildfire as a catalyst for hydrologic and geomorphic change. *Environ. Sci. Oxf.* https://doi.org/10.1093/OBO/9780199363445-0112 (2019).
41. Liu, Z., Ballantyne, A. P. & Cooper, L. A. Biophysical feedback of global forest fires on surface temperature. *Nat. Commun.* **10**, 214. https://doi.org/10.1038/s41467-018-08237-z (2019).
42. Tang, R., Huang, X., Zhou, D. & Ding, A. Biomass-burning-induced surface darkening and its impact on regional meteorology in eastern China. *Atmos. Chem. Phys.* **20**, 6177–6191. https://doi.org/10.5194/acp-20-6177-2020 (2020).

43. Pellegrini, A. F. A., Reich, P. B., Hobbie, S. E. & Coetsee, C. Soil carbon storage capacity of drylands under altered fire regimes. *Nat. Clim. Change* **13**(10), 1–6. https://doi.org/10.1038/s41558-023-01800-7 (2023).
44. Martins, F. S. R. V., Xaud, H. A. M., dos Santos, J. R. & Galvão, L. S. Effects of fire on above-ground forest biomass in the northern Brazilian Amazon. *J. Trop. Ecol.* **28**(6), 591–601. https://doi.org/10.1017/S0266467412000636 (2012).
45. Smith, J. K. In Wildland fire in ecosystems: Effects of fire on fauna. General Technical Report, RMRS-GTR-42-Volume 1 (ed Kapler, S. J.) 83 (U.S. Department of Agriculture, Forest Service, Rocky Mountain Research Station, 2000).
46. Huang, L., Lin, W., Li, F., Wang, Y. & Jiang, B. Climate impacts of the biomass burning in Indochina on atmospheric conditions over Southern China. *Aerosol Air Qual. Res.* **19**, 2707–2720. https://doi.org/10.4209/aaqr.2019.01.0028 (2019).
47. Adámek, M., Hadincová, V. & Wild, J. Long-term effect of wildfires on temperate *Pinus sylvestris* forests: Vegetation dynamics and ecosystem resilience. *For. Ecol. Manag.* **380**, 285–295. https://doi.org/10.1016/j.foreco.2016.08.051 (2016).
48. Pulido-Chavez, M. F. et al. Rapid bacterial and fungal successional dynamics in first year after chaparral wildfire. *Mol. Ecol.* **32**(7), 1685–1707. https://doi.org/10.1111/mec.16835 (2022).
49. Ferrenberg, S. et al. Changes in assembly processes in soil bacterial communities following a wildfire disturbance. *ISME J.* **7**(6), 1102–1111. https://doi.org/10.1038/ismej.2013.11 (2013).
50. Taboada, A., García-Llamas, P., Fernández-Guisuraga, J. M. & Calvo, L. Wildfires impact on ecosystem service delivery in fire-prone maritime pine-dominated forests. *Ecos. Serv.* **50**, 101334. https://doi.org/10.1016/j.ecoser.2021.101334 (2021).
51. Lecina-Diaz, J., Martínez-Vilalta, J., Alvarez, A., Vayreda, J. & Retana, J. Assessing the risk of losing forest ecosystem services due to wildfires. *Ecosys.* **24**, 1687–1701. https://doi.org/10.1007/s10021-021-00611-1 (2021).
52. Vukomanovic, J. & Steelman, T. A systematic review of relationships between mountain wildfire and ecosystem Services. *Landsc. Ecol.* **34**, 1179–1194. https://doi.org/10.1007/s10980-019-00832-9 (2019).
53. Stevens-Rumann, C. & Morgan, P. Repeated wildfires alter forest recovery of mixed-conifer ecosystems. *Ecol. Appl.* **26**(6), 1842–1853. https://doi.org/10.1890/15-1521.1 (2016).
54. Govt. of India. Accessed on 3 May 2024; https://rajyasabha.nic.in/rsnew/official_sites/statelegis.asp.
55. Govt. of India. Accessed on 2 June 2024; https://www.india.gov.in/india-glance/profile.
56. NASA. Accessed on 25 September 2024. https://www.earthdata.nasa.gov/faq/firms-faq#:~:text=For%20MODIS%2C%20the%20confidence%20value,fire)%20to%20all%20fire%20pixels.
57. Wolfe, R., Nishihama, M. & Kuyper, J. MODIS Geolocation status. MODIS Science Team meeting Calibration Breakout Session, NASA GSFC Code 619, accessed on 2 February 2024; https://modis.gsfc.nasa.gov/sci_team/meetings/201304/presentations/calibration/wolfe.pdf (2013).
58. Csiszar, I. & Schroeder, W. Short-term observations of the temporal development of active fires from consecutive same-day ETM+ and ASTER imagery in the Amazon: Implications for active fire product validation. *IEEE J. Sel. Top. Appl. Earth Obs. Remote Sens.* **1**(4), 248–253 (2008).
59. Cooperative Institute for Research in the Atmosphere. https://rammb2.cira.colostate.edu/wp-content/uploads/2020/01/VIIRS_Active_Fire_Quick_Guide_v1-2022.pdf.
60. Dickinson, M. B. et al. Measuring radiant emissions from entire prescribed fires with ground, airborne and satellite sensors–RxCADRE 2012. *Int. J. Wildland Fire* **25**, 48–61. https://doi.org/10.1071/WF15090 (2015).
61. Boschetti, L. & Roy, D. P. Defining a fire year for reporting and analysis of global interannual fire variability. *J. Geophys. Res.* **113**, G03020. https://doi.org/10.1029/2008JG000686 (2008).
62. Sen, P. K. Estimates of the regression coefficient based on Kendall's. *J. Am. Stat. Assoc.* **63**, 1379–1389 (1968).
63. Helsel, D. R. & Hirsch, R. M. Statistical methods in water resources. U.S. Geological survey technique of water resources investigations. Book 4, chapter A3, p 524 (2002).
64. Salmi, T., Määttä, A., Anttila, P., Ruoho-Airola, T. & Amnell, T. *Detecting trends of annual values of atmospheric pollutants by the Mann-Kendall test and Sen's slope estimates-the excel template application MakeSens* (Finnish Meteorological Institute, 2002).
65. Ward, J. H. Jr. Hierarchical grouping to optimize an objective function. *J. Am. Stat. Assoc.* **58**, 236–244 (1963).
66. Global Forest Watch. Accessed on 18 September 2024, https://www.globalforestwatch.org/dashboards/country/IND/?category=fires.
67. Indian Institute of Remote Sensing. Accessed on 10 May 2025. https://www.iirs.gov.in/iirs_slide_page?s=121.
68. Roberts, G., Wooster, M. J. & Lagoudakis, E. Annual and diurnal African biomass burning temporal dynamics. *Biogeosciences* **6**, 849–866. https://doi.org/10.5194/bg-6-849-2009 (2009).
69. Vadrevu, K. & Lasko, K. Intercomparison of MODIS AQUA and VIIRS I-band fires and emissions in an agricultural landscape-implications for air pollution research. *Remote Sens.* **10**, 978. https://doi.org/10.3390/rs10070978 (2018).
70. Department of Agriculture and Framers Welfare. Accessed on 23 May 2024. https://agriwelfare.gov.in/Documents/CropSituation/crops_13012023.pdf.
71. Directorate of Rice Development. Accessed on 1 May 2024. https://drdpat.bih.nic.in/Status%20Paper%20-%2002.htm.
72. Forest Survey of India. Accessed on 3 April 2024. http://vanagniportal.fsiforestfire.gov.in/fsi_fire/fire.html.
73. Balasubramanian, A. Major Forest Areas in India. Technical Report, University of Mysore, India (2017). https://doi.org/10.13140/RG.2.2.17863.70563.
74. Reddy, C. S. et al. Nationwide assessment of forest burnt area in India using Resourcesat-2 AWiFS data. *Curr. Sci.* **112**(7), 1521–1532. https://doi.org/10.18520/cs/v112/i07/1521-1532 (2017).
75. Bahuguna, V. K. & Upadhay, A. Forest fires in India: Policy initiatives for community participation. *Int. For. Rev.* **4**(2), 122–127. https://doi.org/10.1505/IFOR.4.2.122.17446 (2002).
76. North Eastern Space Applications Centre (NESAC). Forest Fire Assessment in Northeast India. North Eastern Space Applications Centre, Dept. of Space, Govt. of India, Meghalaya, India (2014).
77. Forest Survey of India. Accessed on 1 February 2024. http://vanagniportal.fsiforestfire.gov.in/fsi_fire/fire.html.
78. Yadav, K., Escobedo, F. J., Thomas, A. S. & Johnson, N. G. Increasing wildfires and changing sociodemographics in communities across California, USA. *Int. J. Disaster Risk Reduct.* **98**, 104065. https://doi.org/10.1016/j.ijdrr.2023.104065 (2023).
79. Radeloff, V. C. et al. Rapid growth of the US wildland-urban interface raises wildfire risk. *PNAS* **115**(13), 3314–3319. https://doi.org/10.1073/pnas.1718850115 (2018).
80. Kramer, H. A., Mockrin, M. H., Alexandre, P. M. & Radeloff, V. C. High wildfire damage in interface communities in California. *Int. J. Wildland Fire* **28**(9), 641–650. https://doi.org/10.1071/WF18108 (2018).
81. Chen, B. et al. Wildfire risk for global wildland–urban interface areas. *Nat. Sust.* **7**, 474–484. https://doi.org/10.1038/s41893-024-01291-0 (2024).
82. Bikkina, S. et al. Air quality in megacity Delhi affected by countryside biomass burning. *Nat. Sust.* **2**, 200–205. https://doi.org/10.1038/s41893-019-0219-0 (2019).
83. Majumdar, D. Spatial distribution and temporal variation of biomass burning and surface black carbon concentrations during summer (2015–2021) in India. *Air Qual. Atmos. Health* **16**, 459–476. https://doi.org/10.1007/s11869-022-01284-y (2022).
84. Yang, X., Zhao, C., Yang, Y., Yan, X. & Fan, H. Statistical aerosol properties associated with fire events from 2002 to 2019 and a case analysis in 2019 over Australia. *Atmos. Chem. Phys.* **21**, 3833–3853. https://doi.org/10.5194/acp-21-3833-2021 (2021).
85. Fan, H. et al. The role of primary emission and transboundary transport in the air quality changes during and after the COVID-19 lockdown in China. *Geophys. Res. Lett.* **48**(7), e2020GL091065. https://doi.org/10.1029/2020GL091065 (2021).
86. Yang, X., Zhao, C., Yang, Y. & Fan, H. Long-term multi-source data analysis about the characteristics of aerosol optical properties and types over Australia. *Atmos. Chem. Phys.* **21**, 3803–3825. https://doi.org/10.5194/acp-21-3803-2021 (2021).

87. Tonini, M. M., Pereira, M. G., Parente, J. & Orozco, C. V. Evolution of forest fires in Portugal: From spatiotemporal point events to smoothed density maps. *Nat. Haz.* **85**, 1489–1510. https://doi.org/10.1007/s11069-016-2637-x (2016).

Acknowledgements
The author acknowledges use of VIIRS standard fire products data from the archives of NASA's Fire Information for Resource Management System (FIRMS), a part of NASA's Earth Observing System Data and Information System (EOSDIS). The author is sincerely thankful to Director, NEERI for all the encouragement and support extended for carrying out the research work. Manuscript number assigned by the Knowledge Resource Centre (KRC) of CSIR-NEERI is CSIR-NEERI/KRC/2024/OCT/KZC/1.

Author contributions
D.M. developed study concept and design, undertook data extraction, mining and analysis, did all interpretation and GIS-related analyses, solely handled first draft preparation and all subsequent revisions. D.M. read and approved the final manuscript.

Declarations

Competing interests
The author declares no competing interests.

Additional information
Correspondence and requests for materials should be addressed to D.M.

Reprints and permissions information is available at www.nature.com/reprints.

Publisher's note Springer Nature remains neutral with regard to jurisdictional claims in published maps and institutional affiliations.